Contents lists available at ScienceDirect

Digital Chinese Medicine

journal homepage: http://www.keaipublishing.com/dcmed

Lantana camara alleviating TNBS-induced ulcerative colitis in rats: regulating TNF-α/EGFR/STAT3/Bcl-2 signaling pathways

Manoj S. Magre, Pooja A. Bhalerao, Satish K. Mandlik, Deepa S. Mandlik*

Bharati Vidyapeeth (Deemed to be University), Poona College of Pharmacy, Pune, Maharashtra 411038, India

ARTICLE INFO

Article history
Received 22 February 2025
Accepted 14 May 2025
Available online 25 June 2025

Keywords
Ulcerative colitis
Lantana camara
Tri-nitrobenzene sulfonic acid
Network pharmacology
Molecular docking
Inflammatory cytokines

ABSTRACT

Objective To investigate the therapeutic potential and underlying mechanism of *Lantana camara* ethanolic extract (LCEE) in ulcerative colitis (UC).

Methods Phytochemical analysis of LCEE was conducted using qualitative analysis, liquid chromatography-mass spectrometry (LC-MS), and high-performance thin-layer chromatography (HPTLC). The active constituents of LCEE were identified through network pharmacology analysis, followed by molecular docking. The therapeutic mechanism was validated in a UC rat model using 42 male Wistar rats (200 – 250 g) induced by 2,4,6-trinitrobenzene sulfonic acid (TNBS). Rats were randomly divided into seven groups (n = 6 per group): normal control (NC), ethanol control (EC), disease control (DC), three doses of LCEE treatment [low dose LCEE (100 mg/kg), medium dose LCEE (200 mg/kg), and high dose LCEE (400 mg/kg), p.o.], and dexamethasone (DEX, 2 mg/kg, p.o.) groups. Following TNBS-induced UC (120 mg/kg, intrarectally), rats were treated orally for 28 d. Disease severity was assessed through body weight changes, disease activity index (DAI), colon weight, colon length, and morphological scores. Haematological parameters, enzymatic antioxidants, nitric oxide (NO), myeloperoxidase (MPO), and inflammatory cytokines were measured in the serum and colon tissues. Gene expressions of tumor necrosis factor (TNF)-α, epidermal growth factor receptor (EGFR), signal transducer and activator of transcription 3 (STAT3), and B-cell lymphoma 2 (Bcl-2) were analyzed by quantitative reverse transcription polymerase chain reaction (qRT-PCR). Histopathological alterations in the colon tissues were evaluated using hematoxylin and eosin (HE), Giemsa, and periodic acid-schiff staining (PAS).

Results LC-MS analysis identified 13 phytoconstituents in LCEE, and HPTLC analysis confirmed the presence of ursolic acid, geniposide, and chlorogenic acid. Network pharmacological analysis identified 152 potential therapeutic targets with TNF, STAT3, Bcl-2, albumin (ALB), and EGFR as the top 5 hub targets. Molecular docking revealed strong binding affinities of LCEE phytoconstituents with key inflammatory and apoptotic targets: linaroside with TNF-α (– 6.1 kcal/mol), ursolic acid with STAT3 (– 6.8 kcal/mol) and Bcl-2 (– 8.7 kcal/mol), and cirsiliol with EGFR (– 8.2 kcal/mol), comparable to DEX. LCEE treatment significantly increased body weights and thymus weight, while significantly reducing colon weight, spleen weight, and DAI scores. Haematological parameters showed significant improvements with increased haemoglobin, red blood cells, and platelet count, and decreased white blood cells counts. Antioxidants markers were significantly improved with increased glutathione, superoxide dismutase, and catalase levels, and decreased malondialdehyde levels. LCEE

*Corresponding author: Deepa S. Mandlik, E-mail: deepa.mandlik@bharatividyapeeth.edu.

Peer review under the responsibility of Hunan University of Chinese Medicine.

DOI: 10.1016/j.dcmed.2025.05.009

Citation: MAGRE MS, BHALERAO PA, MANDLIK SK, et al. *Lantana camara* alleviating TNBS-induced ulcerative colitis in rats: regulating TNF-α/EGFR/STAT3/Bcl-2 signaling pathways. Digital Chinese Medicine, 2025, 8(2): 234-253.

significantly reduced NO and MPO levels and inflammatory cytokines including TNF-α, interleukin (IL)-1β, nuclear factor kappa-B (NF-κB), IL-6, and IL-12 compared with TNBS treated rats. LCEE downregulated the gene expression levels of TNF-α, EGFR, and STAT3, while upregulating Bcl-2 expression level, indicating modulation of inflammation and apoptosis pathways. Histological evaluation confirmed that after LECC treatment, mucosal ulcers and inflammatory cell infiltration decreased.

Conclusion The findings suggest that *Lantana camara* may serve as a medicinal plant to alleviate UC and offer an investigational basis for the clinical utilization of *Lantana camara*.

1 Introduction

Inflammatory bowel disease (IBD) is a chronic, immune-mediated disorder of the gastrointestinal tract, primarily driven by an abnormal immune response to gut microbiota [1], with two major forms of ulcerative colitis (UC) and Crohn's disease (CD), which differ in location and depth of inflammation [2]. UC is confined to mucosa and submucosa of colon and rectum, whereas CD can affect any part of the gastrointestinal tract with transmural involvement. UC symptoms include diarrhoea, abdominal pain, rectal bleeding, and weight loss [3]. Although its etiology remains unclear, genetic, environmental, and immune factors are implicated. Oxidative stress, cytokine dysregulation, and immune cell activation (e.g., $CD8^+$ $IL\text{-}17^+$ T cells) are central to UC pathophysiology [4]. Effective management involves modulating inflammatory mediators such as cytokines and myeloperoxidase (MPO) [5].

The goals of pharmacological treatment for UC are to minimize flare-up symptoms and stop them from recurring. Oral 5-aminosalicylic acid is presently the main treatment for patients with mild to severe UC [6]. Additional treatment options include corticosteroids like prednisolone, immunosuppressive medications like azathioprine and methotrexate, monoclonal antibodies, and tumour necrosis factor (TNF) inhibitors like infliximab and adalimumab. However, the existing treatments for UC are connected with side effects, patient variability in effectiveness, and possible long-term harm including nephrotoxicity, myelosuppression, and cardiovascular problems [7]. The advancement of novel botanical remedies, conventional herbal formulations, as well as medications derived from herbal flora to improve the treatment of UC is gaining interest [8]. As a result, identifying novel compounds and preparing medications derived from medicinal plants may offer a valuable method for uncovering phytomedicine strategies aimed at treating UC [9].

Lantana camara (*L. camara*), a widely distributed ornamental plant, has a long-standing history in traditional medicine for treating various ailments. Its therapeutic applications include antimicrobial, anti-inflammatory, analgesic, antioxidant, antipyretic, gastrointestinal relief, respiratory conditions, and wound healing properties [10]. The plant's medicinal efficacy is largely attributed to its rich phytochemical composition, encompassing flavonoids, saponins, tannins, and alkaloids. These bioactive compounds have been shown to mitigate inflammatory responses and neutralize free radicals, thereby reducing oxidative stress [11]. Notably, oleanolic acid, a triterpenoid extracted from the roots of *L. camara*, has demonstrated significant anti-inflammatory and hepatoprotective activities. The current investigation tries to evaluate the beneficial advantages of *L. camara* in the therapy of UC in light of its ethnomedical usage in several gastrointestinal illnesses [12]. *L. camara*, commonly known as "Red Sage" or "Spanish Flag", is an ornamental plant with colorful flowers and aromatic leaves, often regarded as an "ornamental weed" [13]. Additionally, it is acknowledged as an ornamental plant species and is extensively used to treat various illnesses. According to previous studies, extracts from *L. camara* are used in old-style medicine for the treatment of a diversity of conditions, including eczema, measles, cancer, rheumatism, malaria, ulcers, asthma, swellings, tumours, catarrhal infections, high blood pressure and tetanus [14-16]. Leaves are used to cure rheumatism, ulcers and cuts in Asian nations.

The plant's traditional use in treating inflammatory diseases is further supported by research that has found more bioactive triterpenoids inside with anti-inflammatory properties [17]. *L. camara* has long been used to treat digestive issues in relation to gastrointestinal health. Methanolic extracts of *L. camara* leaves have been shown to have anti-ulcerogenic properties, which lends scientific support to its application in the treatment of duodenal and stomach ulcers [18]. Moreover, *L. camara's* antioxidant properties are important for shielding the digestive system from oxidative stress, which is a cause of inflammatory bowel disorders. The components of the plant may preserve mucosal integrity and support general gut health by scavenging dangerous free radicals. Including *L. camara* in treatment plans provides a natural way to treat inflammatory diseases, especially those that impact the digestive tract. Its complex pharmacological effects are consistent with traditional medicine's holistic tenets, which place an emphasis on equilibrium and the body's natural capacity for healing.

Although *L. camara* has long been used in traditional

medicine for gastrointestinal disorders, its anti-ulcerative mechanisms remain poorly understood. This study aims to evaluate the anti-inflammatory effects of *L. camara* ethanolic extract (LCEE) in UC using both *in vivo* and *in silico* approaches.

2 Materials and methods

2.1 Network pharmacological analysis of *L. camara*

2.1.1 Data mining and screening of phytoconstituents of *L. camara* The phytoconstituents of *L. camara* were searched with IMPPAT 2.0 database (https://cb.imsc.res.in/imppat/). PubChem database (https://pubchem.ncbi.nlm.nih.gov/) was searched for baseline on each phytoconstituent, including Canonical SMILES and three-dimensional (3D) conformer structures, which were saved in structure data format (SDF) format. The study utilized screening filters with oral bioavailability ⩾ 30% and drug-likeness ⩾ 0.18 to enhance drug development. *L. camara* active phytoconstituents were used for target prediction using online tools like BindingDB (https://www.bindingdb.org/rwd/bind/chemsearch/marvin/FMCT.jsp) with the similarity threshold of 0.85 and Swiss target prediction (https://www.swisstargetprediction.ch/) with the species set to "homo sapiens" and "probability > 1".

2.1.2 ADMET analysis Furthermore, to evaluate the pharmacokinetic properties and drug-likeness of the screened active compounds, absorption, distribution, metabolism, excretion, and toxicity (ADMET) analysis was performed. This step ensured that only compounds with favorable pharmacological profiles were considered for subsequent molecular docking studies. The ADMET predictions were conducted using SwissADME.

2.1.3 Acquisition of UC targets The investigation was carried out with "ulcerative colitis" in DisGeNET (https://www.disgenet.org/) and GeneCards (https://www.genecards.org/) databases for disease-related targets. Integrating the identified targets and eliminating redundant targeted to focus on the ones that are pertinent to UC.

2.1.4 Target prediction and validation To enhance understanding of UC, target prediction was performed. The target proteins of active phytoconstituents were modified to their standard gene names utilizing UniProt Knowledge database (https://www.uniprot.org/). Official gene symbols were found by looking up the target protein names in UniProtKB, with "homo sapiens" as the organism's designation.

2.1.5 Intersection of phytoconstituent targets and UC targets The Venny 2.1 web-based tool (https://bioinfogp.cnb.csic.es/tools/venny/) was used to combine the *L. camara* phytoconstituents and UC targets, identifying common targets. To see the connection between these targets, a Venn diagram was made. These intersecting targets were potential for the therapeutic effects of *L. camara* on UC.

2.1.6 Protein-protein interaction (PPI) network construction The PPI network was created by importing the overlapping targets into Search Tool for the Retrieval of Interacting Genes/Proteins (STRING) 11.0 (https://stringdb.org/cgi/input?sessionId=bdx7uARsfd8Y&input_page_show_search=on) database, evaluating the protein interaction, imagining the obtained PPI network by Cytoscape 3.9.1, and filter the primary targets by network topological investigation. To identify genes in Cytoscape, three topological measures were computed for each node: degree, betweenness centrality, and closeness centrality. A node's degree indicated how many neighbours it has. Betweenness centrality measured the frequency of node-link to the shortest path between two nodes. By calculating the distance between each node in the PPI network, closeness centrality evaluated a node's significance.

2.1.7 Enrichment analysis by Gene Ontology (GO) and Kyoto Encyclopedia of Genes and Genomes (KEGG) GO is a widely used tool for annotating genes and their expression products. It is mostly separated into three categories: biological process (BP), cellular components (CC), molecular functions (MF). KEGG pathway enrichment analysis was also conducted. ShinyGO v0.741 (http://bioinformatics.sdstate.edu/go74/) was used for GO and KEGG analysis. From a macro viewpoint, KEGG enrichment analysis may provide the functional details of a large number of genes and forecast the underlying drug-disease signaling pathway.

2.2 Molecular docking analysis

As per the liquid chromatography-mass spectrometry (LC-MS) and enrichment analysis results and the comprehensive analysis of the current research status, we designated the most important phytoconstituents of LCEE. The 3D structure of these phytoconstituents was downloaded in SDF from the PubChem database (https://pubchem.ncbi.nlm.nih.gov/). The 3D structures were retrieved from PDB Database (https://www.rcsb.org/). The docking simulation was performed with selected key proteins by AutoDock Vina v1.2.5 (https://vina.scripps.edu). The docking minimum free energy was used to predict the binding affinity between chemicals and proteins. The higher the affinity, the smaller the free energy. Dexamethasone (DEX), a standard anti-inflammatory drug, was used as a reference compound to benchmark the binding affinities of LCEE phytoconstituents. The docking results were visualized using BIOVIA Discovery Studios (https://discover.3ds.com/discovery-studio-visualizer-download) and PyMOL 3.1 (https://www.pymol.org/).

2.3 *In vitro* cytotoxicity assay of LCEE

The 3-(4,5-dimethylthiazol-2-yl)-2,5-diphenyltetrazolium bromide (MTT) reduction test was employed to assess the Caco-2 cell viability. The countess automated cell counter (Invitrogen, USA) was utilized to count the Caco-2 cells. These cells were then plated in a 96-well plate at a density of 2×10^4 cells/well. The cells were seeded, allowed to incubate for 24 h, and then exposed to varying doses of LCEE (0, 100, 200, 300, 400, 500, 600, 700, 800, 900, and 1 000 μg/mL). Each well received 10 μL of MTT solution [5 mg/mL in phosphate buffer saline (PBS)] after 24 h incubation. Following that, the plate was maintained in a humidified incubator with 5% CO_2 at 37 °C for 3 h. The liquid removal from the wells, 100 μL of dimethyl sulfoxide (DMSO) was included to dissolve the formazan salt that had formed. The optical density was measured at 517 nm using a microplate reader (Synergy HTX, Biotek, USA). To confirm the studies' repeatability, three distinct biological replications were conducted.

2.4 *In vivo* experimental validation

2.4.1 Botanical material and extract preparation The *L. camara* leaves were collected, washed with distilled water thrice, and dried for 4 d in a shade. The plant was recognized and verified (authentication certificate No. BSI/WRC/Tech./2023/09) by the Botanical Survey of India, Ministry of Environment and Forest, Government of India, Pune. Briefly, the shade-dried leaves were crushed and 100 g powder was extracted with 1 000 mL of ethanol: water (90 ∶ 10 v/v) by maceration method. After 72 h, the liquid extract was filtered and concentrated using a rotary evaporator at 20 °C under a vacuum to get LCEE. The yield of LCEE was found to be 15.47%. The LCEE was preserved for further research at – 10 °C [19].

2.4.2 Preliminary phytochemical screening of LCEE Preliminary phytochemical analysis of the LCEE was tested using tannins and phenolics (5% ferric chloride, diluted nitric acid, and lead acetate), alkaloids (tannic acid, Hager's test and Wagner's test), glycosides (Baljeet's test, Legal's test, and Killer-killani test), flavonoids (sulphuric acid test) and carbohydrates (Molisch's test) [20].

2.4.3 LC-MS analysis of LCEE LC-MS was utilized to detect active constituents in the LCEE. Liquid chromatography-electrospray ionization-mass spectrometry (LC-ESI-MS) tests were carried out at the sophisticated analytical instrument facility, in Pune. The acetonitrile extracts were centrifuged for 5 min at 10 000 rpm before analysis. The equipment used for high-performance liquid chromatography (HPLC) consisted of an automated injector and two pumps. An Agilent SyncronisTM C18 silica column (100 mm × 4.6 mm, 5 μm) was used for the chromatographic splitting, and it was heated to 30 °C. A – 0.1% formic acid in water and B-90% acetonitrile in water were mobile phases, and the flow rates were 0.8 mL/min. The mass range of mass spectrometry was 50 – 1 000 atomic mass units, and it was operated in both positive and negative ESI modes. Specific configurations comprised a gas temperature of 250 °C, a fragment voltage of 135 V, a nebulizer pressure of 55 psi, a drying gas flow rate of 10 L/min, and a sheath gas temperature of 250 °C. The capillary voltage (VCap) was set at 3 500 V for both positive and negative ESI modes. With a 5 μL injection volume, the entire run took 15 min. The data acquisition was processed by Agilent MassHunter Workstation Software LC/MS Data Acquisition for 6 400 Series Triple Quadrupole vB.07.01, and the acquired data was processed by Agilent MassHunter Workstation Software Qualitative Analysis vB.07.00.

2.4.4 High-performance thin layer chromatography (HPTLC) analysis of LCEE Pre-activated (100 °C) silica gel F_{254} HPTLC plates (10 cm × 10 cm; 0.25 mm layer thickness; Merck) were used for chromatography. The analysis was carried out using thin layer chromatography (TLC) visualizer 3 and reflectance spectrometer TLC scanner 3 (CAMAG), which had a monitoring range of 190 – 700 nm. The data processing and acquisition were done with the software Win CATS 3.2.2. A total of 10 μL of samples were applied to plates using a Linomat 5 automated TLC applicator (CAMAG) with nitrogen flow, forming 8 mm broad bands positioned 8 mm at the plate bottom. The delivery rate from the syringe was kept at 10 μL/s. For 25 min, TLC plates were developed in a Camag twin trough glass tank that was pre-saturated with the mobile phase. This allowed the solvent to rise to a height of eight centimetres at ambient temperature. The mobile phase for the ursolic acid detection was toluene ∶ acetone ∶ formic acid (7.8 ∶ 2.2 ∶ 0.15). After dipping the plates in anisaldehyde sulfuric acid reagent for 5 s, they were heated to 110 °C for 10 – 15 min, or until spots were visible. For geniposide, the mobile phase was ethyl acetate ∶ methanol ∶ water (7 ∶ 3 ∶ 0.3), whereas toluene ∶ ethyl acetate ∶ methanol ∶ water ∶ formic acid (3 ∶ 6 ∶ 0.5 ∶ 0.5 ∶ 1) was the mobile phase for chlorogenic acid.

2.4.5 Animals Global Bioresearch Solutions Pvt. Ltd. provided the 42 specific pathogen-free (SPF) male Wistar albino rats (weighing 200 – 250 g). Throughout the experimental period, they were kept in a controlled setting with a 12-h light/dark cycle with unlimited access to food and water. The surrounding air was maintained at 20 ± 2 °C with a relative humidity of 30% – 70%. The institutional animal ethics committee of Poona College of Pharmacy approved the experimental protocol (PCP/IAEC/2023/4-1) with the registration number 1703/PO/Re/S/13/CPCSEA.

2.4.6 Drugs and reagents The colorectal adenocarcinoma cell line (Caco-2 cells) (HTB-37 ATCC) was purchased from the American-type culture collection, USA.

Trypsin, minimum essential medium eagle's (MEM), and antibiotic-antimycotic solution were bought from Himedia Laboratories, Mumbai. TNBS (TCI, India), ethanol (Labnol, India), O-dianisidine hydrochloride, DTNB, DEX, thiobarbituric acid, hexadecyltrimethylammonium bromide (HTAB), Griess reagent, DMSO and MTT (Sigma Aldrich, USA), fetal bovine serum (NextGen life sciences private limited, Delhi), adrenaline bitartrate, thiobarbituric acid, and trichloroacetic acid (LOBA Chem Pvt. Ltd.) were purchased. The kits for hemospot (Biolab diagnostics, India), interleukin (IL)-6, IL-1β, TNF-α, IL-12, nuclear factor kappa-B (NF-κB), EGFR, STAT3, and Bcl-2 (Krishgen Biosystem, Mumbai), and complete blood count (Span Diagnostics, India) were obtained. The analytical-grade reagents and chemicals were bought from local suppliers.

2.4.7 Induction of UC and LCEE treatment UC was induced in rats using a well-established TNBS-induced colitis model with slight modifications [21]. Prior to induction, animals were fasted for 24 h with free access to water. Under light anesthesia with thiopentone sodium (40 mg/kg, i.p.), a flexible catheter (external diameter 2 mm) was gently inserted 8 cm into the rectum. A single dose of TNBS (120 mg/kg) dissolved in 50% ethanol (total volume 0.25 mL) was slowly instilled intrarectally to induce colitis. Following administration, animals were held in a head-down position for 2 – 3 min to ensure uniform distribution of the TNBS solution throughout the colon.

At 24 h post-induction (day 1), oral treatment began and continued once daily for 28 d. Rats were randomly assigned to seven groups (n = 6 per group): (i) normal control (NC) group: received 0.2 mL of distilled water intrarectally on day 0, with no further treatment; (ii) ethanol control (EC) group: received 0.25 mL of 50% ethanol intrarectally on day 0; (iii) disease control (DC) group: received a single intrarectal dose of TNBS (120 mg/kg in 50% ethanol) on day 0 without subsequent treatment; (iv) low-dose LCEE group: received TNBS on day 0, followed by LCEE 100 mg/kg orally once daily for 28 d; (v) medium-dose LCEE group: received TNBS on day 0, followed by LCEE 200 mg/kg orally once daily for 28 d; (vi) high-dose LCEE group: received TNBS on day 0, followed by LCEE 400 mg/kg orally once daily for 28 d; (vii) DEX group: received TNBS on day 0, followed by dexamethasone 2 mg/kg orally once daily for 28 d.

On day 29, animals were anesthetized using thiopentone sodium (40 mg/kg, i.p.) for blood sample collection via retro-orbital puncture. Serum was separated by centrifugation and stored at – 80 °C for biochemical analyses. Subsequently, the animals were sacrificed with an overdose of thiopentone sodium (70 mg/kg, i.p.), and organs including the colon, spleen, and thymus were harvested, cleaned, and weighed. Colon tissues were divided for histological, biochemical, and gene expression studies, and stored accordingly. The overall experimental design and treatment timeline are illustrated in Figure 1.

2.4.8 Determination of body weight, relative organ weight, colon weight, and colon length Rats' body weight was measured for 28 d. The weights of spleen and thymus gland were recorded at the end of the experiment (day 29). Finally, colon length and colon weight were measured to assess the severity of UC.

2.4.9 Disease activity index (DAI) and macroscopic evaluation of colon The rats were weighed and tested for behavioral changes, bloody stool, and stool consistency every day [22]. The scoring for DAI calculation is given in Table 1. The severity of UC was evaluated by an unbiased evaluator who was unaware. Each animal had its distal

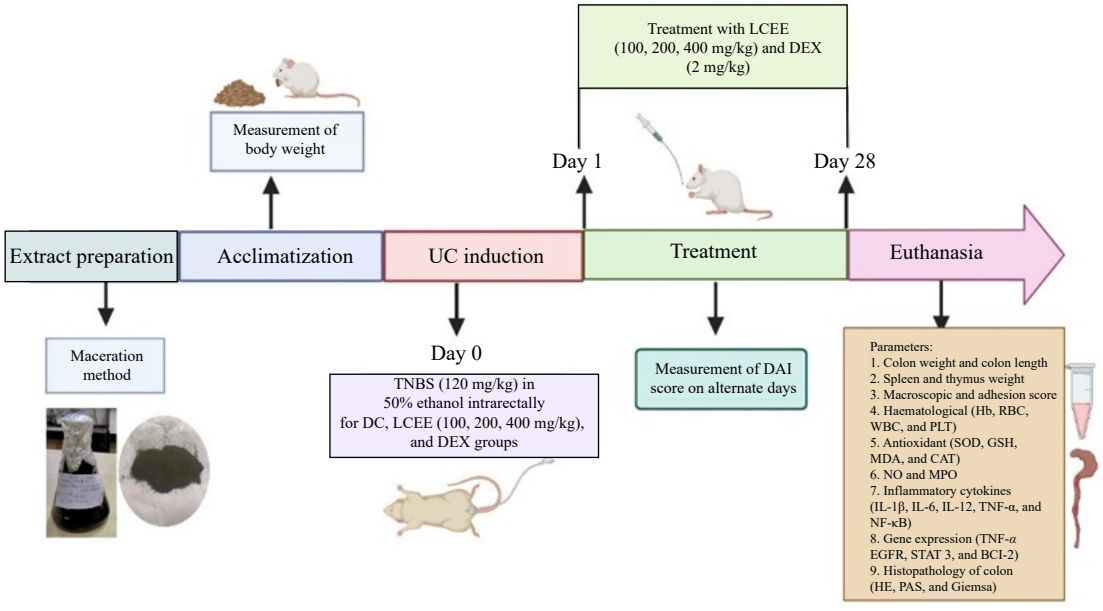

Figure 1 Experimental procedure of UC and treatment protocol with LCEE and DEX

8 cm of colon dissected, cut longitudinally, and cleaned in physiological saline to get rid of any faeces, and it was then evaluated. Using a microscope, the colons were examined, and any visible injury was graded on a scale of 0 – 4 by predetermined standards [21]. A scale of 0: no damage; 1: central hyperaemia without ulcers; 2: ulceration without hyperaemia or thickening of the gut wall; 3: ulceration with worsening at one site; and 4: two or more significant areas of inflammation and ulceration, or one significant area of inflammation and ulceration extending > 1 cm along the colon was used to assign scores for macroscopic inflammation. The criteria set by BOBIN-DUBIGEON et al. [23] were used to evaluate occurrence of adhesions score (score 0 – 2): 0 (no adhesion), 1 (moderate adhesion), and 2 (major adhesion).

Table 1 Criteria for scoring DAI

Score	Weight loss (%)	Stool consistency	Occult blood or gross bleeding
0	None	Normal	Negative
1	1 – 5	Loose	Negative
2	5 – 10	Loose	Hemoccult positive
3	10 – 15	Diarrhea	Hemoccult positive
4	> 15	Diarrhea	Gross bleeding

2.4.10 Determination of blood parameters Complete blood cell kits (Span Diagnostics, India) were used to analyze the blood parameters. Haemoglobin (Hb), white blood cells (WBC), red blood cells (RBC), and platelet counts (PLTs) were measured from blood samples by using an automated haematological analyser.

2.4.11 Determination of *in vivo* antioxidant activity The Marklund and Marklund method was employed to ascertain superoxide dismutase (SOD) activity [24]. The Sedlak and Lindsay procedure determined colon homogenate's malondialdehyde (MDA) levels [25]. EBRAHIMPOUR et al. [26] method was used to measure glutathione (GSH) levels. Catalase (CAT) activity was assessed by the method of SADAR et al. [27].

2.4.12 Determination of myeloperoxidase The MPO level was assessed in colon samples using a technique outlined by KRAWISZ et al. [28]. Colonic segments were homogenized in a solution comprising 50 mmol/L sodium phosphate (pH 6.0), and 0.5% HTAB. This substance works as a detergent to break up MPO-containing neutrophil granules. After homogenization, the mixture was centrifuged for 10 min at 4 °C. The samples were then frozen and thawed three times to encourage the disruption of cellular structures and the release of enzymes. After extracting a volume of 50 μL from the supernatant, 150 μL of reaction buffer-which includes hydrogen peroxide, o-dianisidine hydrochloride, and 50 mmol/L phosphate buffer was added. The results were expressed as MPO units per gram of tissue and the absorbance was determined at 450 nm.

2.4.13 Determination of nitric oxide (NO) Using the Griess reagent, tissue NO levels were determined as total nitrite/nitrate [29]. Following a 10% homogenate produced by homogenizing colon tissue in 50 mmol/L potassium phosphate buffer (pH 7.8), the samples were centrifuged at 11 000 × g for 15 min at 4 °C. 100 μL of the supernatant and 100 μL of Griess reagent were combined for experiment. The sample was incubated for 10 min, and the absorbance was determined at 540 nm.

2.4.14 Determination of pro-inflammatory cytokines Enzyme-linked immunosorbent assay (ELISA) kits (Krishgen Biosystem, Mumbai) were used to quantify the serum levels of IL-6, TNF-α, IL-1β, IL-12, and NF-κB following the manufacturer's instructions.

2.4.15 Gene expression analysis by quantitative reverse transcription polymerase chain reaction (qRT-PCR) qRT-PCR was used to assess the impact of LCEE on the mRNA expression levels of TNF-α, EGFR, STAT3, and Bcl-2 in the colon tissue of rats given TNBS. In summary, TRIzol reagent was used to isolate RNA, which was subsequently processed with RNase-free DNase and measured. (Supplementary Table S1) Using the primer set and SYBR Green master mix, 2 μg of pure RNA were reverse transcribed into cDNA for amplification. The resulting amplification data were normalized to GAPDH as a housekeeping gene.

2.4.16 Histopathological analysis The tissues from the colon had embedded in paraffin, and treated with formalin. The processed colon tissues were sectioned into 5 μm slices, stained for histological observations using hematoxylin and eosin (HE), periodic acid-schiff, and Geimsa staining, and examined under 40 × magnification under a microscope [30].

2.5 Statistical analysis

The data were represented as mean ± standard error of the mean (SEM). Using GraphPad Prism v5.0, statistical analysis was carried out using two-way analysis of variance (ANOVA) followed by Bonferroni's post hoc test for recurrent measures and one-way ANOVA followed by Tukey's multiple comparison test for the last-day parameters. $P < 0.05$ was considered statistically significant.

3 Results

3.1 Network pharmacology of *L. camara*

3.1.1 Identification and screening of *L. camara* phytoconstituents A total of 13 active phytoconstituents were selected from LC-MS/MS analysis of LCEE: ursolic acid, oleanolic acid, geniposide, theveside, verbascoside, icterogenin, lantic acid, cirsiliol, chlorogenic acid, linaroside, catechin gallate, narcissin, and betulinic acid with oral bioavailability ⩾ 30% and drug-likeness ⩾ 0.18 as

screening parameters based on the ADMET profile by using SwissADME database (http://www.swissadme.ch/index.php). These 13 phytoconstituents were selected for further investigation.

3.1.2 Screening of potentially therapeutic targets of *L. camara* for UC After merging and eliminating duplicates, 13 phytoconstituents of 152 targets were gathered from BindingDB and Swiss target prediction database, and 3 713 UC-associated genes were collected from the DisGeNET and GeneCards databases to find possible treatment targets for UC by *L. camara* screening. After comparing these disease-related targets with *L. camara* putative targets, 100 genes were found to overlap. These overlapping genes were thought to be possible targets for *L. camara* for the treatment of UC (Figure 2A).

3.1.3 Phytoconstituent-target network analysis Using Cytoscape 3.9.1, 152 possible targets and 13 active components of *L. camara* for the management of UC were imported to create a Phytoconstituent-Target network. The resulting network represented medications through dark green and hexagon shape nodes, active components through light green and oval shape nodes, and common targets through light green and rectangle shape nodes (Figure 2B).

3.1.4 Construction of PPI network and drug phytoconstituents-targets-disease network By entering 100 targets into the STRING database, a PPI network was created (Figure 2C). The data was then imported into Cytoscape 3.9.1 for network visualization and topology analysis. The PPI network contained 99 nodes and 857 edges. Using Cytoscape, the interactions between these 100 targets were examined. These targets were identified as crucial *L. camara* targets against UC. Supplementary Table S2 displays a list of 100 important targets together with comprehensive information. The top five important targets of PPI network with the highest degree value were determined to be TNF, STAT3, Bcl-2, ALB, and EGFR, which were the main targets of *L. camara* in the management of UC. Further, GO enrichment analysis revealed that the overlapping targets were significantly involved in

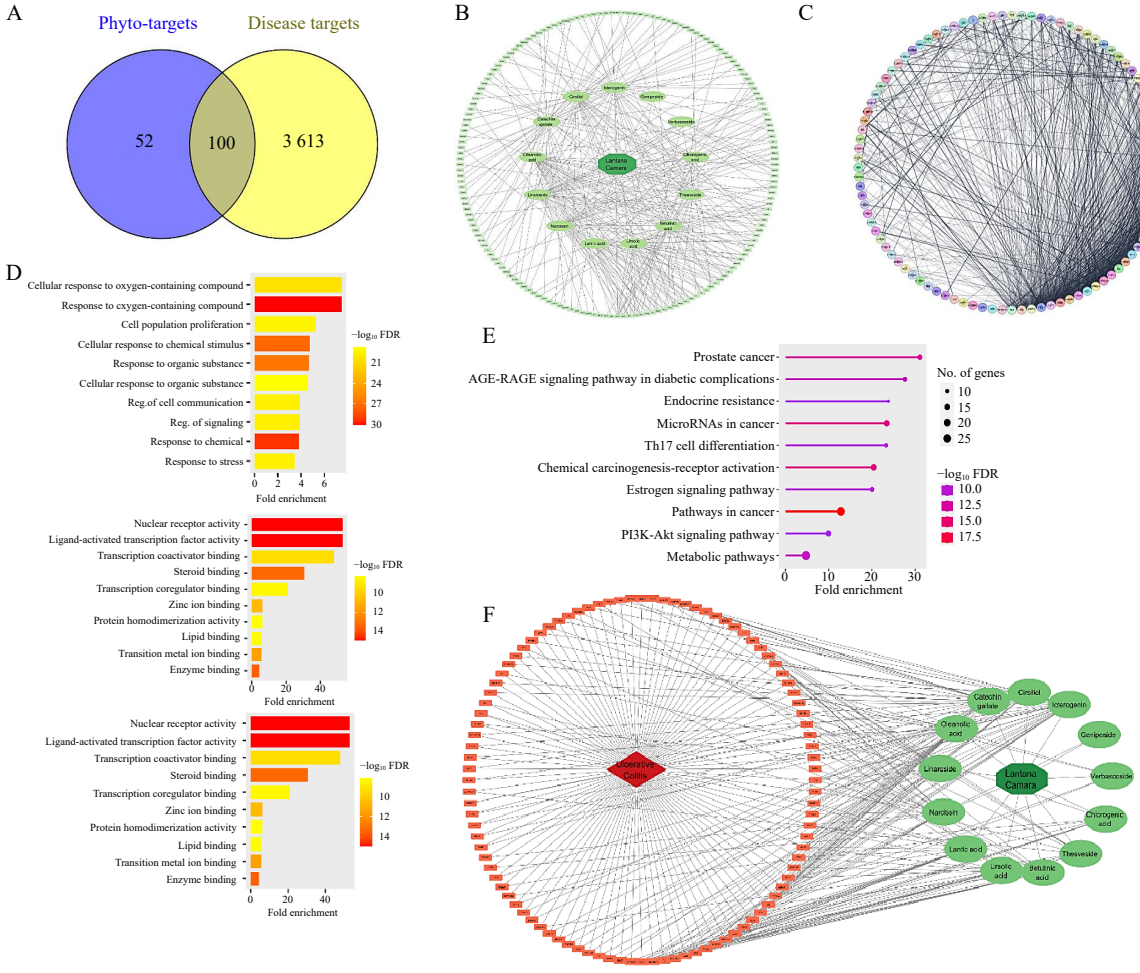

Figure 2 Network pharmacology analysis of LCEE against UC

A, Venn diagram showing common targets between LCEE phytoconstituents and UC-related genes. B, phytoconstituent-target network showing interactions between active compounds of LCEE and predicted protein targets. C, PPI network of overlapping targets. D, GO enrichment analysis of key targets (biological process, cellular component, molecular function). E, KEGG pathway enrichment analysis of common targets. F, compound-target-pathway network linking LCEE components to UC pathways via predicted targets.

key biological processes such as cellular response to chemical stimulus, response to organic substances, regulation of cell communication, response to stress, and cell population proliferation. Molecular function analysis indicated significant enrichment in nuclear receptor activity, ligand-activated transcription factor activity, transcription coactivator binding, and zinc ion binding. The KEGG pathway enrichment analysis demonstrated that the targets were mainly associated with pathways relevant to ulcerative colitis pathology, including PI3K-Akt signaling pathway, Estrogen signaling pathway, Th17 cell differentiation, AGE-RAGE signaling pathway, and pathways in cancer, indicating potential mechanisms through which *L. camara* may exert its therapeutic effects in UC (Figure 2D and 2E). As shown in Figure 2F, red colour rectangle shapes were the common targets of disease and phytoconstituents and the green colour octagon and oval shape are *L. camara* and its phytoconstituents.

3.2 Molecular docking of LCEE phytoconstituents

AutoDock Vina was used to confirm the molecular docking (Figure 3). The findings demonstrated that ursolic acid, oleanolic acid, cirsiliol, linaroside, and DEX exhibited the lowest binding free energies. The key targets EGFR, Bcl-2, TNF, and STAT3 were used to identify the binding affinities of the compounds (Supplementary Table S3). In docking, the binding energy was used to compare the docked conformation to reference or other docked conformations. The chemical structure, binding energies, inhibitory constants, and bond lengths of these phytoconstituents with each of the proteins are listed in Supplementary Table S4.

3.3 Effects of LCEE on cell viability of Caco-2 cells

Caco-2 cells were treated with several doses of LCEE (100 to 1 000 μg/mL) for 24 h to check the cytotoxicity. Cell viability in the control cell (without LCEE treatment) was considered 100%. Then, percentage viability at other concentrations was calculated. Based on the MTT assay results shown in Figure 4A, Caco-2 cells maintained over 85% – 90% viability at LCEE concentrations ranging from 100 to 800 μg/mL. However, at 900 μg/mL and above, a marked decrease in viability was observed, with viability dropping to approximately 65% at 900 μg/mL and around 50% at 1 000 μg/mL. The IC_{50} value was found to be approximately 980 μg/mL, indicating that LCEE is relatively non-toxic up to moderate concentrations.

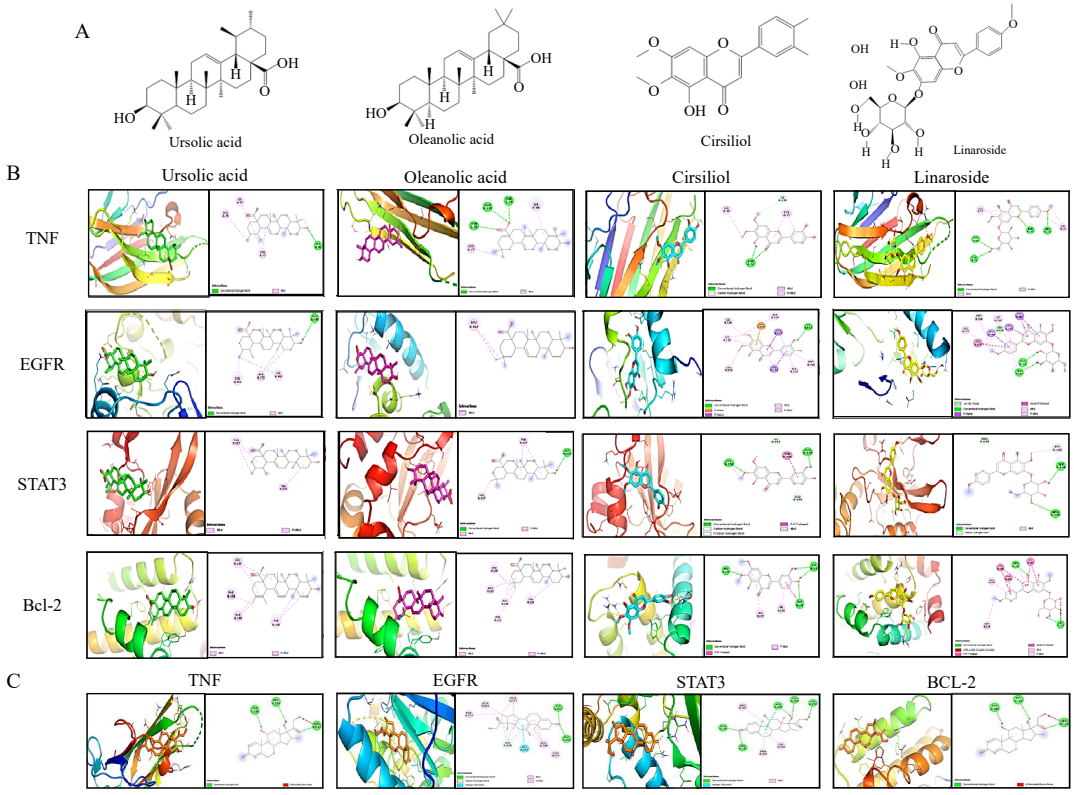

Figure 3 Molecular docking interactions of active LCEE phytoconstituents and DEX with key inflammatory/apoptotic targets

A, structures of active phytoconstituents of LCEE: ursolic acid, oleanolic acid, linaroside, and cirsiliol. B, 2D and 3D docking interaction of LCEE constituents with TNF, EGFR, STAT3, and Bcl-2, respectively. C, 2D and 3D interaction of DEX with TNF, EGFR, STAT3, and Bcl-2 for comparison with LCEE. Docking energies indicate strong binding affinity of LCEE compounds, comparable to standard DEX. Color codes represent different bond types.

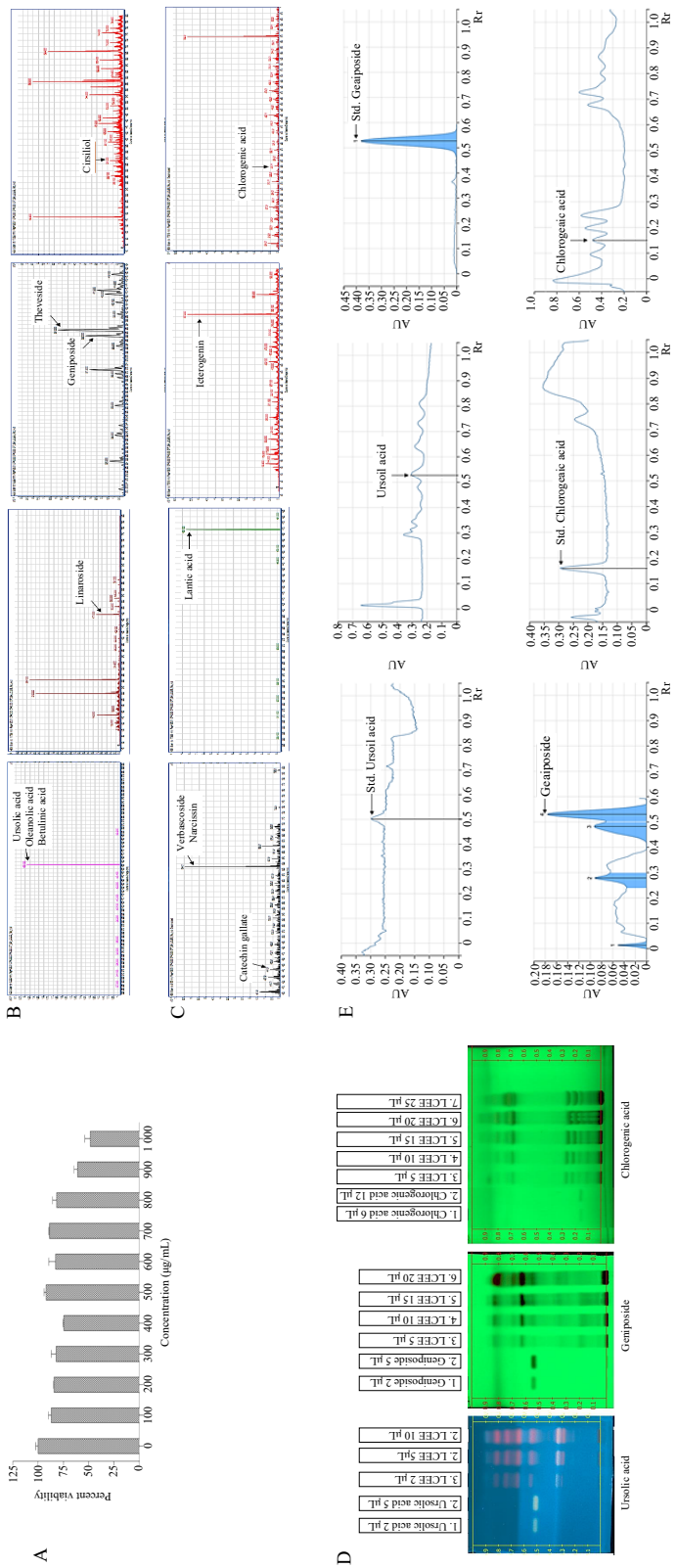

Figure 4 LC-MS, HPTLC, and cytotoxicity profiling of LCEE

A, cytotoxicity effect of LCEE on Caco-2 cell viability assessed via MTT assay. B, LC-MS chromatogram (positive ESI mode) showing identification of key phytoconstituents including cirsiliol, oleanolic acid, betulinic acid, etc. C, LC-MS chromatogram (negative ESI mode) identifying verbascoside, narcissin, chlorogenic acid, etc. D, HPTLC fingerprint profiling of LCEE for ursolic acid, geniposide, and chlorogenic acid compared with standards. E, spectral overlay and Rf value comparisons between LCEE and standards, confirming compound presence.

3.4 LC-MS analysis of LCEE

The LCEE was analyzed by LC-MS, which demonstrated the existence of numerous bioactive constituents with diverse retention times. Figure 4B chromatograms showed that cirsiliol, oleanolic acid, theveside, betulinic acid, geniposide, ursolic acid, and linaroside were identified in LCEE in positive ESI mode based on their retention time and m/z ratio. Figure 4C chromatograms showed that icterogenin, catechin gallate, verbascoside, narcissin, lantic acid, and chlorogenic acid were identified in LCEE in negative ESI mode based on their retention time and m/z ratio. A total of 13 compounds were found in LCEE by using LC-MS analysis (Supplementary Table S5).

3.5 HPTLC analysis of LCEE

The LCEE was standardized by HPTLC fingerprinting, and the standard ursolic acid, geniposide, and chlorogenic acid spots were matched with LC spots by TLC visualizer 3, respectively (Figure 4D and 4E), and scanned with TLC scanner 3 at 366, 242, and 254 nm. The Rf values were found to be ursolic acid (0.52), geniposide (0.53), and chlorogenic acid (0.16). The compounds were found in the LCEE. The spectral analysis for standard and LCEE revealed the identity of standard in the LCEE, qualitatively alike HPTLC fingerprinting was conquered for LCEE.

3.6 Preliminary phytochemical screening of LCEE

The phytochemical analysis of LCEE exhibited the presence of tannins, phenolics, alkaloids, glycosides, flavonoids, and carbohydrates. The outcomes of preliminary phytochemical screening of LCEE are shown in Table 2.

3.7 Effects of LCEE on colon morphology, colon macroscopic score, and adhesion score in TNBS-induced UC rats

The rats in NC and EC groups showed no signs of necrosis, haemorrhage, or inflammation when compared with DC group rats (Figures 5A – 5C). Following the intra-rectal administration of TNBS, the DC rats exhibited symptoms indicative of UC, including mucosal necrosis, ulceration, erosion, bleeding, and inflammation (Figure 5D). Comparing the oral administration of LCEE at different doses of 100, 200, and 400 mg/kg with DC group rats, erosion, necrosis, ulceration, and inflammation were considerably inhibited (Figures 5E – 5I). Furthermore, in comparison with DC rats, oral administration of DEX (2 mg/kg) substantially prevented the TNBS-induced, bleeding, inflammation, and ulcer (Figure 5J).

The colon macroscopic and adhesion score of DC rat was considerably enlarged when related to NC rats ($P < 0.001$). However, in comparison with the DC rats, the administration of LCEE (100, 200, and 400 mg/kg) and DEX (2 mg/kg) displayed a substantial decrease in the colon macroscopic and adhesion score ($P < 0.05$, $P < 0.01$, or $P < 0.001$) (Figure 5B and 5C).

3.8 Effects of LCEE on body weight, spleen weight, thymus weight, colon weight, colon length, and DAI in TNBS-induced UC rats

At day 0, there was no noticeable change observed between the body weights of the DC and NC rats. The rats treated with DEX (2 mg/kg) and LCEE (100, 200, and 400 mg/kg) showed no substantial change in body weight at day 0. When TNBS was administered intrarectally, the body weight of DC rats reduced considerably ($P < 0.001$) from day 7 in comparison with NC rats. In contrast, rats treated with LCEE at doses of 100, 200, and 400 mg/kg exhibited a substantial increase in body weight after 14 d as compared with DC rats ($P < 0.05$, $P < 0.01$, or $P < 0.001$). From day 14, the rats treated with DEX (2 mg/kg) exhibited a noteworthy rise in body weight in comparison with DC rats ($P < 0.01$ or $P < 0.001$) (Figure 5D).

The spleen and thymus weights of DC rats were considerably increased ($P < 0.001$), compared with those of NC rats after intra-rectal treatment of TNBS. Nevertheless, spleen and thymus weights were considerably decreased in rats treated with LCEE (100, 200, and 400 mg/kg)

Table 2 Preliminary phytochemical screening of LCEE

No.	Class	Test	Result	Color
1	Tannins and phenolics	5% ferric chloride	Positive	Black
		Diluted nitric acid	Positive	Yellow
		Lead acetate	Positive	White precipitate
2	Alkaloids	Tannic acid	Positive	Buff
		Hager's test	Positive	Yellow precipitate
		Wagner's test	Positive	Reddish brown
3	Glycosides	Baljeet's test	Positive	Yellow
		Legal's test	Positive	Red ring
		Killer-killani test	Positive	Greenish bluish
4	Flavanoids	Sulfuric acid test	Positive	Yellow
5	Carbohydrates	Molisch's test	Positive	Violet ring

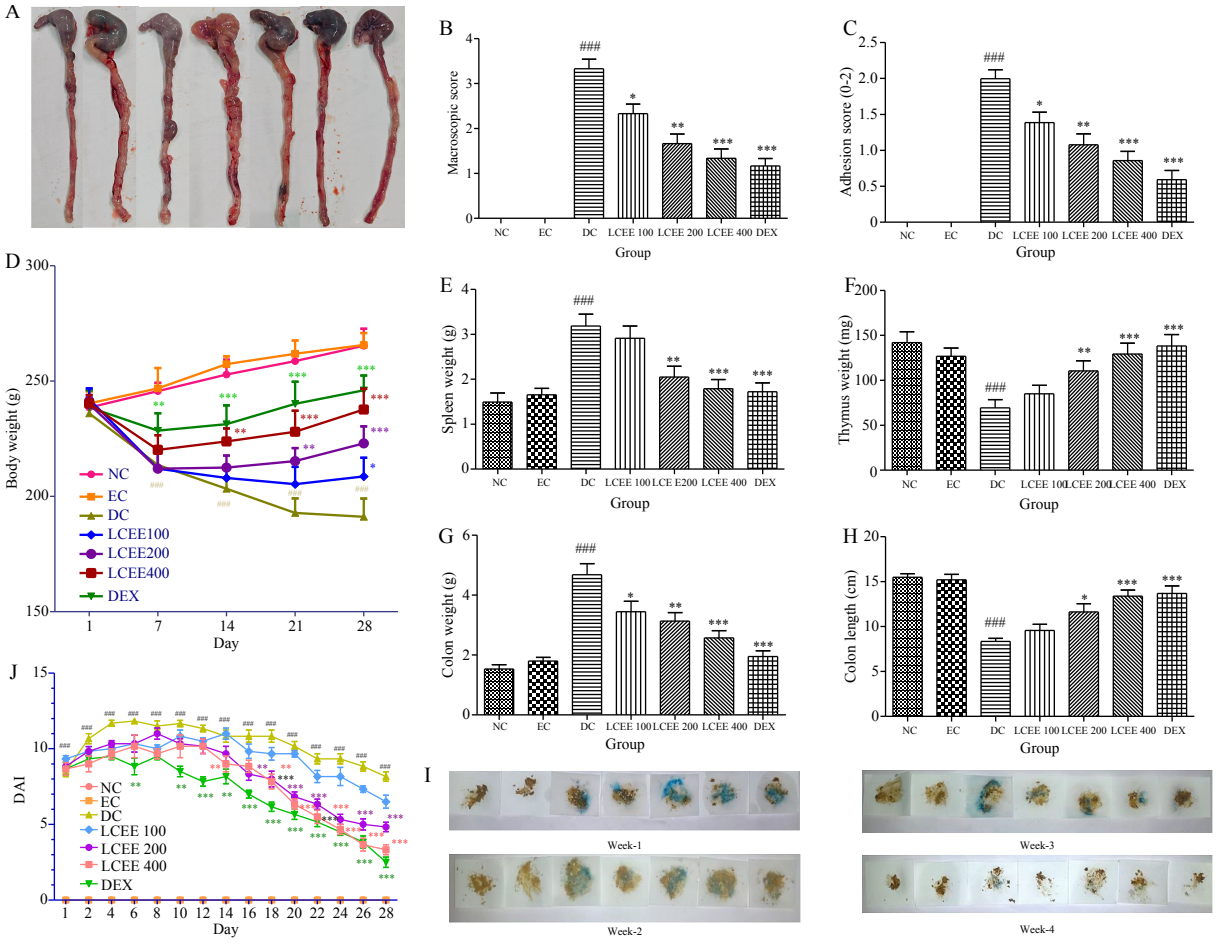

Figure 5 Protective effects of LCEE on gross morphology and clinical indicators in TNBS-induced UC rats

A, representative colon images on day 29 across experimental groups. From left to right: NC, EC, DC, LCEE 100, LCEE 200, LCEE 400, and DEX groups. B, colon macroscopic score. C, adhesion score. D, changes in body weight. E, spleen weight. F, thymus weight. G, colon weight. H, colon length. I, weekly fecal occult blood test (from left to right: NC, EC, DC, LCEE 100, LCEE 200, LCEE 400, and DEX groups). J, DAI scores. Data were represented as mean ± SEM ($n = 6$). Data were analysed by two-way ANOVA, followed by Bonferroni's test for body weight and one-way ANOVA, and followed by Tukey's multiple comparison test. $^{###}P<0.001$, compared with NC group. $^{*}P < 0.05$, $^{**}P < 0.01$, and $^{***}P < 0.001$, compared with DC group.

than in DC group ($P < 0.01$ or $P < 0.001$). Rats administered with DEX (2 mg/kg) had a significantly lower spleen and thymus weight ($P < 0.001$) in comparison with DC group rats (Figure 5E and 5F).

The colon weight of the DC rats was substantially increased and colon length was significantly decreased than that of the NC rats following intra-rectal TNBS treatment ($P < 0.001$). And colon weight was significantly lowered ($P < 0.01$ or $P < 0.001$) and colon length was significantly increased ($P < 0.05$ or $P < 0.001$) in rats treated with LCEE treatment (100, 200, and 400 mg/kg) than in the DC rats. Moreover, the rats treated with DEX (2 mg/kg) exhibited a substantial reduction in colon weight and a rise in colon length than in DC group rats ($P < 0.001$) (Figure 5G and 5H).

Figure 5I exhibited a weekly representation of faecal occult blood in TNBS-induced UC in rats. When TNBS was administered intra-rectally to rats, the DAI score decreased considerably ($P < 0.001$) in comparison with NC rats. However, rats administered with LCEE (100, 200, and 400 mg/kg) and DEX (2 mg/kg) had considerably lower DAI from day 14 when compared with DC group rats ($P < 0.01$ or $P < 0.001$) (Figure 5J).

3.9 Effects of LCEE on haematological parameters, antioxidant markers, MPO, and NO in TNBS-induced UC rats

PLT, RBC, and Hb count in DC rats were considerably decreased as related to those in NC rats after intra-rectal administration of TNBS ($P < 0.001$). Nevertheless, compared with DC rats, those treated with LCEE (100, 200, and 400 mg/kg) and DEX (2 mg/kg) showed a noticeable increase in PLT, Hb, and RBC counts ($P < 0.01$ or $P < 0.001$). The WBC count of DC group rats, i.e. TNBS control was significantly improved as matched to NC rats ($P < 0.001$). However, the treatment of rats with LCEE (100, 200, and 400 mg/kg) and DEX (2 mg/kg) considerably increased the WBC count as linked to DC rats ($P < 0.05$, $P < 0.01$ or $P < 0.001$) (Figures 6A – 6D).

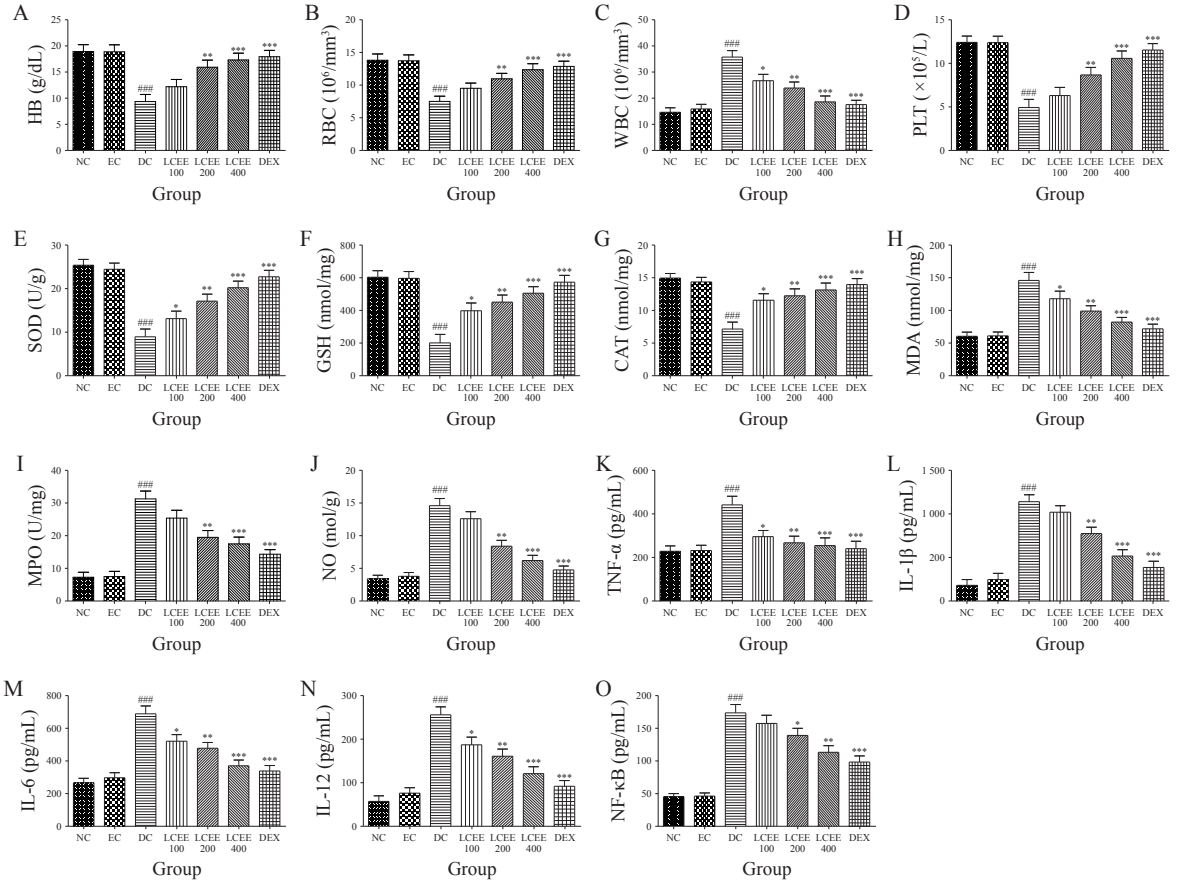

Figure 6 Effects of LCEE on haematological, antioxidant, inflammatory, and oxidative stress markers in TNBS-induced UC rats

A, Hb. B, RBC. C, WBC. D, PLT. E, SOD. F, GSH. G, CAT. H, MDA. I, MPO. J, NO. K, TNF-α. L, IL-1β. M, IL-6. N, IL-12. O, NF-κB. Data were represented as mean ± SEM (n = 6), and one-way ANOVA was used for analysis followed by Tukey's multiple comparison test. $^{###}P < 0.001$, compared with NC group. $^{*}P < 0.01$, $^{**}P < 0.01$, and $^{***}P < 0.001$, compared with DC group.

Colitis induction brought about a substantial reduction in SOD, GSH, and CAT concentration in the colon tissue and a significant increase in the MDA level of DC rats as compared with NC rats ($P < 0.001$). The LCEE (100, 200, and 400 mg/kg) treatment in rats considerably increased the levels of colonic SOD, GSH, and CAT concentration and considerably lowered the MDA concentration in comparison with DC rats ($P < 0.05$, $P < 0.01$, or $P < 0.001$, respectively). However, the treatment of rats with DEX (2 mg/kg) exhibited a substantial restoration of colonic antioxidant stress markers in comparison with the DC group rats ($P < 0.001$) (Figure 6E – 6H).

The rats treated with TNBS demonstrated a substantial ($P < 0.001$) rise in MPO and NO levels in comparison with NC rats. However, the treatment of rats with LCEE (100, 200, and 400 mg/kg) and DEX (2 mg/kg) considerably decreased the MPO and NO levels in comparison with NC rats ($P < 0.01$ or $P < 0.001$) (Figure 6I and 6J).

3.10 Effects of LCEE on inflammatory cytokines in TNBS-induced UC rats

As shown in Figure 6K – 6O, the UC induced by intrarectal administration of TNBS in rats, caused a substantial ($P < 0.001$) increase of TNF-α, IL-1β, IL-6, IL-12, and NF-κB levels as compared with NC rats. Whereas, the treatment of rats with LCEE (100, 200, and 400 mg/kg) displayed substantial ($P < 0.05$, $P < 0.01$, or $P < 0.001$) reduction in TNF-α, IL-1β, IL-6, IL-12, and NF-κB levels while DEX (2 mg/kg) treated to rats also displayed substantial ($P < 0.001$) reduction in TNF-α, IL-1β, IL-6 IL-12, and NF-κB when compared with DC rats.

3.11 Effects of LCEE on gene expression levels by qRT-PCR in TNBS-induced UC rats

The expression levels of TNF-α, EGFR, STAT3, and Bcl-2 was determined by qRT-PCR technique. The expression levels of TNF-α, EGFR, and STAT3 was considerably improved and Bcl-2 gene was decreased in rats treated with TNBS as compared with the NC group rats ($P < 0.001$). After the treatment of rats with LCEE (100, 200, and 400 mg/kg), the expression levels of TNF-α, EGFR, and STAT3 was significantly decreased and Bcl-2 genes were significantly increased as related to the TNBS group rats ($P < 0.05$, $P < 0.01$, or $P < 0.001$). Likewise, the DEX-treated rats also exhibited a substantial reduction in the TNF-α, EGFR, and STAT3 gene level and a substantial rise in the Bcl-2 expression level when linked with TNBS-treated rats ($P < 0.001$) (Figure 7A – 7D).

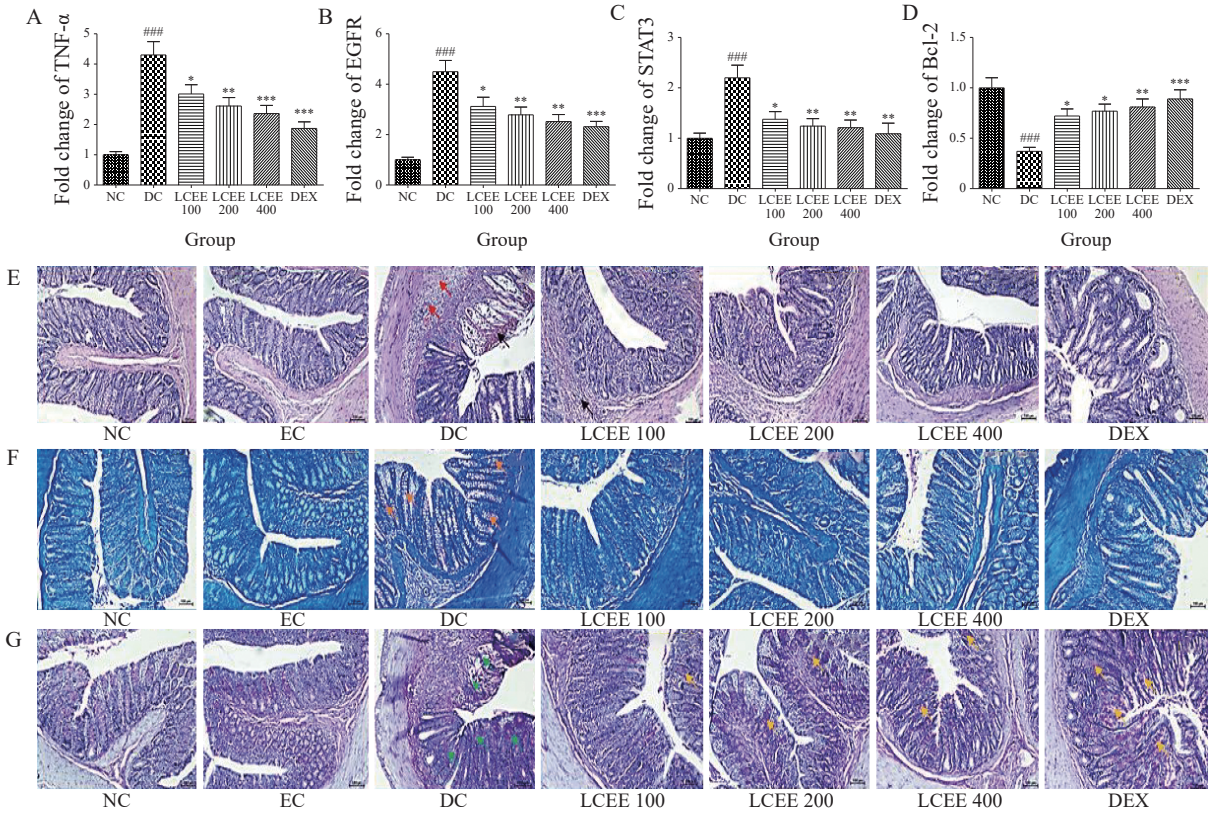

Figure 7 Gene expression and histopathological effects of LCEE in TNBS-induced UC rats

A – D, RT-PCR analysis of TNF-α, EGFR, STAT3, and Bcl-2 mRNA expression in colon tissue, respectively. E, HE staining showing colonic architecture LCEE restored mucosal integrity. F, Giemsa staining depicting inflammatory cell infiltration in colon tissue. G, PAS staining revealing goblet cell damage and epithelial restoration after LCEE treatment. Data were represented as mean ± SEM (n = 6) and analyzed utilizing one-way ANOVA followed by Tukey's multiple comparison test. $^{###}P < 0.001$, compared with NC group. $^{*}P < 0.01$, $^{**}P < 0.01$, and $^{***}P < 0.001$, compared with DC group. HE staining: infiltration of inflammatory cells (red arrow), necrosis of the mucosal layer (black arrow). Giemsa staining: presence of inflammatory cells (orange arrow). PAS staining: damage to the epithelium layer and loss/ absence/ injury of goblet cells (green arrow), and restoration of the epithelium layer and goblet cells (orange arrow).

3.12 Effects of LCEE on HE, Giemsa, and PAS staining in TNBS-induced UC rats

3.12.1 HE staining The colon tissue from NC and EC rats showed a normal microscopic architecture upon histological analysis. There was no inflammatory cell infiltration, the intestinal cytoarchitecture seemed normal, and the epithelial cell layer was intact. Whereas, significant disruption of the normal architecture of colon, infiltration of inflammatory cells, and necrosis of the mucosal layer were seen in TNBS-treated rats. In comparison with DC (TNBS-treated) rats, the rats treated with LCEE (100 mg/kg) exhibited restoration of mucosal architecture but inflammatory cell infiltration was observed. However, in rats treated with LCEE (200 and 400 mg/kg), and DEX (2 mg/kg) exhibited significant inhibition of TNBS-induced colonic damage in the colon samples (Figure 7E).

3.12.2 Geimsa staining The histological examination of colon tissue samples of NC and EC group rats exhibited no architectural disturbances and absence of inflammatory cells. Whereas, DC rats revealed a significant presence of inflammatory cells. However, rats treated with LCEE (100, 200, and 400 mg/kg) displayed a dose-dependent reduction of inflammatory cells. DEX (2 mg/kg) treatment in rats showed a considerable decrease in the accumulation of inflammatory cells (Figure 7F).

3.12.3 PAS staining The structural architecture of the colon tissue epithelium layer appears to be normal in the rats in NC and EC groups. However, damage to the epithelium layer and loss/absence/injury of goblet cells were seen in DC rats. Dose-dependent restoration of the epithelium layer and goblet cells was seen in rats treated with LCEE (100, 200, and 400 mg/kg). However, the rats treated with DEX (2 mg/kg) exhibited epithelium integrity with a normal appearance of goblet cells (orange arrow) (Figure 7G).

4 Discussion

4.1 Therapeutic relevance of LCEE in UC management

The current pharmaceutical management of IBD primarily makes use of corticosteroids, immunosuppressants, biologics, and aminosalicylates. However, these treatments are linked to several adverse outcomes, especially when long-term administration of drugs is necessary.

Additionally, there are cases where patients disregard conventional therapy protocols [31]. As a result, there's been an increase in interest in investigating complementary and alternative medicine as a way to treat UC with better efficacy, safety, and patient adherence [32]. For the treatment of intestinal inflammatory conditions, natural products particular to medicinal plants are widely used as complementary and alternative therapies. Medicinal herbs include a variety of active phytoconstituents that can target different parts of inflammatory pathway simultaneously [33]. Safety-wise, *in vitro* experiments conducted on the Caco-2 cell line demonstrated that LCEE did not result in cytotoxicity to Caco-2 cells. Furthermore, 13 compounds were detected by LC-MS/MS analysis of LCEE among which ursolic acid, geniposide, chlorogenic acid, and oleanolic acid are the most commonly found phytoconstituents and all of them are reported for anti-ulcer properties [34-37]. LC-MS has been employed to perform a preliminary phytochemical screening on various leaf extracts. The results identified multiple classes of phytoconstituents in *L. camara* leaves, including steroids, terpenoids, flavonoids, quinones, carbohydrates, alkaloids, and phenols. These compounds were present in varying proportions, indicating a complex chemical composition within the leaves of *L. camara*. The study's findings suggest that these identified chemicals may contribute to the plant's pharmacological properties and hold significant potential for innovative medical applications.

Integrating traditional Chinese medicine (TCM) concepts into the discussion enhances the understanding of LCEE's therapeutic mechanisms in UC. TCM attributes UC to factors like "spleen deficiency" and "damp-heat accumulation", which disrupt gastrointestinal harmony. LCEE, derived from *L. camara*, is traditionally recognized for "tonifying the spleen and stomach" and "clearing heat and detoxifying", aligning with its observed pharmacological effects [38]. Modern study has shown that many Chinese herbal medicines, including LCEE, exert therapeutic effects in UC by modulating gut microbiota, signaling pathways, and cytokines. This aligns with TCM principle of restoring balance and eliminating pathogenic factors [39]. Furthermore, existed research has been indicated that TCM formulations focusing on "clearing heat and removing toxins" are commonly employed in UC treatment, supporting the integration of these concepts into our discussion [40]. By bridging TCM theories with contemporary scientific findings, we may provide a comprehensive understanding of LCEE's role in UC management, highlighting its potential as a therapeutic agent that harmonizes traditional wisdom with modern medical approaches.

4.2 Target prediction and validation through network pharmacology and molecular docking

Molecular docking tools in this study in conjunction with network pharmacology can significantly improve the LCEE effect on intestinal inflammation in UC [41]. Network pharmacology is a promising method that can be used to uncover the mechanisms of action of herbal extracts. The network pharmacology analysis identified TNF-α, STAT3, EGFR, and Bcl-2 as hub targets with the highest degree centrality values within the PPI network constructed from 100 overlapping genes between UC-related and LCEE-related targets. High-degree nodes in such networks represent proteins with a significant number of direct interactions and are often central regulators of biological processes, particularly those involved in complex diseases like ulcerative colitis. The identification of these hub nodes supports the multi-target mode of LCEE action in UC. For instance, TNF-α is a key upstream pro-inflammatory cytokine that drives downstream signaling cascades, including NF-κB and STAT3 activation. EGFR and STAT3 are central to cell survival, epithelial integrity, and inflammatory gene expression, while Bcl-2 regulates mitochondrial apoptosis. The presence of these high-degree targets indicates that LCEE acts not via a single mechanism but through modulation of multiple interconnected inflammatory and apoptotic pathways. From the ADMET analysis, four compounds namely ursolic acid, oleanolic acid, cirsiliol, and linaroside were found to follow Lipinski Rule of Five, and these compounds are for molecular docking study. High binding affinity was demonstrated via molecular interactions of *L. camara* for TNF protein with linaroside (– 6.1 kcal/mol), for STAT3 protein with ursolic acid (– 6.8 kcal/mol), for EGFR with cirsiliol (– 8.2 kcal/mol), and Bcl-2 with ursolic acid (– 8.7 kcal/mol) with low docking energies, these outcomes were equal to those of DEX, TNF protein (– 7.18 kcal/mol), STAT3 (– 7.98 kcal/mol), EGFR (– 8.41 kcal/mol), and Bcl-2 (– 6.85 kcal/mol). Compounds with low docking energy and high binding affinity for target proteins have been shown in several investigations to potentially therapeutic activity [42]. Furthermore, several phytoconstituents in LCEE (e.g., ursolic acid, linaroside, and cirsiliol) showed high-affinity binding to these targets in molecular docking studies, reinforcing the biological relevance of network findings and highlighting the compound-target-disease interactions in a holistic manner.

LCEE's modulation of the TNF-α/EGFR/STAT3/Bcl-2 axis, we have explicitly distinguished between direct and indirect effects based on the molecular docking data and *in vivo* findings. Specifically, molecular docking analysis revealed that key phytoconstituents within LCEE—namely linaroside, ursolic acid, and cirsiliol—exhibited high binding affinities to TNF-α, Bcl-2, STAT3, and EGFR, respectively. These results suggest direct interactions between the compounds and their target proteins, indicative of potential binding inhibition mechanisms. For example, linaroside showed direct binding to TNF-α with a docking energy of – 6.1 kcal/mol, while ursolic acid

bound directly to Bcl-2 (– 8.7 kcal/mol) and STAT3 (– 6.8 kcal/mol), and cirsiliol to EGFR (– 8.2 kcal/mol). These binding interactions are comparable to those of standard drug DEX. In contrast, the indirect effects of LCEE are observed *in vivo* via downregulation of mRNA expression levels of TNF-α, STAT3, and EGFR, and the upregulation of Bcl-2 expression level. These transcriptional modulations suggest that beyond direct protein binding, LCEE also exerts downstream signaling suppression likely mediated via its antioxidant, anti-inflammatory, and anti-apoptotic actions. This includes attenuation of oxidative stress markers (MDA, MPO, and NO), reduction in pro-inflammatory cytokines (IL-1β, IL-6, IL-12, and NF-κB), and histological recovery of colonic architecture.

4.3 Amelioration of clinical and gross inflammatory manifestations

In current investigation, rats' colons were given TNBS (120 mg/kg) in an ethanol solution by the rectal route, which resulted in the induction of experimental colitis. The intestinal barriers, such as the mucosa, were broken down using ethanol, exposing the colon's innermost layers to TNBS haptenization [43]. TNBS not only damages intestinal mucosa and induces necrotic cell death through pro-oxidant pathways, but it also hinders mucosal healing and induces aberrant immune activation, which in turn drives inflammatory processes [44]. Due to TNBS's disruption of intestinal epithelial cell layers, dehydration, and inadequate nutrition absorption may have contributed to the study's findings of a drop in body weight [45]. The considerable drop in body weight observed in colitis rats was effectively improved by treatment with LCEE. An enlarged spleen is a reliable marker of intestinal inflammation in animal models of UC [46]. The rats treated with TNBS showed a smaller thymus than the NC group rats, which is a crucial immune system regulatory organ. Rats treated with LCEE showed suppressive effects on spleen weight gain in addition to an increase in thymus weight [47].

As previously stated, faecal occult blood, stomach pain, diarrhoea, tenesmus, weight loss, and bloody stools are common clinical symptoms in UC patients [48]. Using this well-established model, we measured the colon length, DAI, colon macroscopic score, and colon histological alterations in rats treated with TNBS. DAI and macroscopic scores indicate the severity of UC brought on by TNBS administration. Rats with high DAI scores have discomfort problems such as diarrhoea, faecal bleeding, and weight loss [49]. The UC colonic mucosa exhibits macroscopic alterations that are ascribed to severe necrosis, oedema, goblet cell hyperplasia, and infiltration of inflammatory cells [50]. The increase in colon weight/colon length ratio is frequently correlated with increases in cell infiltration and oedema [51]. An indirect measure that has an inverse relationship with the degree of UC caused by TNBS is colon length. In comparison with NC rats, the present study found that rats treated with TNBS lost more colon weight, had higher DAI, and macroscopic scores, and shorter colon length. Rats treated with LCEE and DEX showed significant improvements in colon length after UC induction, as well as significant reductions in DAI and macroscopic scores, in comparison with DC rats. This may have been due to a decrease in extreme oedema and inflammatory cell infiltration by the LCEE.

4.4 Haematological stabilization

The most frequent extraintestinal consequence in patients with UC is anaemia [52]. The main causes of anaemia in UC include deficiencies in iron and vitamin B12 brought on by bleeding, poor absorption, shortened absorption times, and low serum protein/albumin levels [53]. Rats are administered with TNBS intra-rectally exhibited decreased Hb, RBC, and PLT counts and increased WBC counts, according to haematological analysis. An elevated WBC count indicates a persistent inflammation and oedema state in the large intestine [54]. In this study, the oral administration of LCEE to rats resulted in a significant increase in the levels of RBC, Hb, and PLT and a reduced number of WBC in rats given TNBS treatment.

4.5 Restoration of antioxidant defense and suppression of oxidative stress markers

One of the most prevalent pathogenic variables causing inflammatory illnesses is oxidative stress, which is also linked to the aetiology of IBD [55]. It has been shown that an excess of reactive oxygen species in intestinal mucosa triggers an immune response that leads to intestinal inflammation, damages intestinal epithelial cells, and jeopardizes the integrity of intestinal barrier. Enzymatic antioxidants, such as SOD, may help to convert O_2^- to O_2, which is then converted to H_2O_2, whereas CAT, an enzyme found in peroxisomes, helps convert H_2O_2 into H_2O and O_2 molecules. Furthermore, GSH, an intracellular non-enzymatic antioxidant, functions as a biomarker for oxidative damage and inflammation [56]. Administration of LCEE significantly elevated levels of SOD, CAT, and GSH in comparison to TNBS-treated rats, verifying the positive effects of LCEE treatment and demonstrating its anti-inflammatory potential. One widely recognized sign of oxidative stress and lipid peroxidation is MDA, a result of the oxidation of polyunsaturated fatty acids [57]. Moreover, higher levels have been seen in the intestinal tissues of TNBS-treated rats [58]. Administration of LCEE significantly decreased the levels of MDA in comparison with TNBS-treated rats by preventing the process of lipid peroxidation, which is the primary factors that initiate the inflammatory pathway from producing free radicals. Therefore, the results of experiment propose that the TNBS-induced UC inflammatory signalling cascade is

disrupted by LCEE treatment in rats. Further, we observed a significant reduction in colonic levels of MPO—a neutrophil-derived enzyme that contributes to oxidative stress and tissue damage [59]. NO, another inflammatory mediator contributing to nitrosative stress and epithelial dysfunction, was also significantly decreased in LCEE-treated rats [60]. These findings highlight the dual role of LCEE in both suppressing oxidative damage and limiting neutrophil-driven inflammation.

4.6 Downregulation of pro-inflammatory cytokines and NF-κB pathway inhibition

The gut immune system is significantly regulated by cytokines. An essential component of the pathogenesis of IBD is pro-inflammatory cytokines [61]. Pro-inflammatory cytokines are produced in excess as a result of leukocytes, including granulocytes, moving to the irritated mucosa and surface ulcers. These cytokines signal the severity of the disease [62]. TNF-α, IL-1β, IL-6, IL-12, and NF-κB are cytokines that promote inflammation [63]. IL-1β can cause a rise in neutrophil counts and encourage neutrophil migration, T cell activation, and survival [64]. In our investigation, TNBS-treated rats has higher serum levels of TNF-α, IL-1β, IL-6, IL-12, and NF-κB, which suggested severe inflammation. Rats treated with the LCEE showed a substantial decrease in the levels of TNF-α, IL-1β, IL-6, IL-12, and NF-κB when compared with TNBS-treated rats. This suggests that the LCEE may inhibit the recruitment of leukocytes and macrophages, which in turn may lower the release of pro-inflammatory cytokines and eventually attenuated inflammation, reducing neutrophil production.

4.7 Transcriptional modulation of target genes supporting multi-modal action

Gene expression studies further substantiated the *in silico* findings. TNBS exposure led to upregulation of TNF-α, EGFR [65, 66], and STAT3 [67], mRNA levels, while LCEE treatment significantly downregulated their expression levels. Conversely, Bcl-2 [68]—a key anti -apoptotic gene —was upregulated by LCEE, indicating a potential protective effect on epithelial cell survival and mucosal healing. Dysregulation of these genes has been associated with disease chronicity and therapeutic resistance in UC, and their normalization further underscores the efficacy of LCEE. Anti-TNF agents like infliximab and adalimumab act primarily by neutralizing TNF-α, a key pro-inflammatory cytokine. Our network pharmacology analysis similarly identified TNF-α as a top hub target of LCEE, indicating an overlapping anti-inflammatory mechanism. However, LCEE also targets additional high-degree nodes such as STAT3, EGFR, and Bcl-2, which are not directly modulated by anti-TNF drugs. These targets are involved in regulating epithelial repair, inflammation, and apoptosis, suggesting that LCEE may exert broader, multi-target effects beyond cytokine neutralization. This comparison highlights that while LCEE shares common pathways with existing biologics, it also modulates unique targets, potentially offering added therapeutic benefits in UC.

4.8 Histological restoration

Histopathological analysis further confirmed the protective role of LCEE in maintaining mucosal integrity. TNBS-treated colons showed extensive epithelial disruption, crypt architectural loss, mucosal ulceration, and infiltration of inflammatory cells, particularly neutrophils and lymphocytes. These pathological changes closely mimic the mucosal damage observed in human (Figure 8).

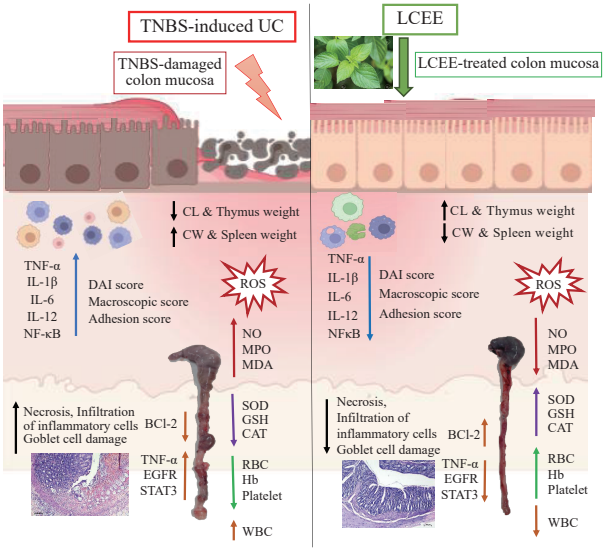

Figure 8 Proposed mechanistic pathway of LCEE in UC: inhibition of TNF-α/STAT3/EGFR axis and upregulation of Bcl-2

4.9 Advantages, limitations, and future research directions

A major advantage of LCEE lies in its multi-targeted mechanism—simultaneously attenuating inflammation, oxidative stress, and apoptosis. Unlike monoclonal antibodies targeting a single cytokine, LCEE exhibits a broader therapeutic spectrum with fewer anticipated side effects. Additionally, the presence of natural antioxidants and safety in Caco-2 cells positions it as a promising candidate for nutraceutical development or adjunctive therapy in IBD. However, there are limitations that warrant consideration. First, long-term safety, toxicity, and pharmacokinetic profiles of LCEE were not evaluated in this study. Second, we failed to assess the impact of LCEE on the gut microbiota, which plays a crucial role in UC pathogenesis and treatment response. Third, the study relied on a single acute colitis model, and findings may differ in chronic or relapsing models. Future directions should include: (i) evaluation of chronic and relapsing UC models; (ii) investigation of gut microbiota modulation by LCEE;

(iii) use of gene knockout and transgenic models to confirm target-specific actions; (iv) testing in human-derived intestinal organoids and clinical samples; (v) comprehensive safety and pharmacokinetic profiling.

5 Conclusion

Our research shows that LCEE may exhibite a protective effect against TNBS-induced UC in rats, indicating that it may serve as a potentially effective candidate for UC treatment. The treatment of rats with LCEE inhibited diarrhoea, lessened weight loss, enhanced the colon weight/colon length ratio of colon, restored haematological and antioxidant markers, lowered MPO and NO levels, improved cytokine levels, gene expression levels, and colon tissue histological alterations. These findings demonstrate LCEE's potential as a plant-based treatment for UC. However, it is imperative to assess the effectiveness of LCEE in alternative animal models of UC before starting clinical trials. The clinical translation of these discoveries would be a viable avenue for future research. Furthermore, more research is necessary to evaluate the long-term positive impacts of LCEE because the current evidence focuses on the short-term animal model of UC.

Acknowledgements

We would like to appreciate Dr. A. P. Pawar, Principal, Poona College of Pharmacy, Bharati Vidyapeeth (Deemed to be University) for providing the necessary facilities to carry out this research work.

Competing interests

The authors declare no conflict of interest.

References

[1] FOKAM TAGNE MA, NOUBISSI PA, GAFFO EF, et al. Effects of aqueous extract of *Anogeissus leiocarpus* (DC) Guill. Et Perr. (Combretaceae) leaves on acetic acid-induced ulcerative colitis in rats. Advances in Traditional Medicine, 2022, 22(3): 631–640.

[2] FOKAM TAGNE MA, TCHOFFO A, NOUBISSI PA, et al. Effects of hydro-ethanolic extract of leaves of *Maesa lanceolata* (Mursinaceae) on acetic acid-induced ulcerative colitis in rats. Inflammopharmacology, 2021, 29(4): 1211–1223.

[3] KAUR A, GOGGOLIDOU P. Ulcerative colitis: understanding its cellular pathology could provide insights into novel therapies. Journal of Inflammation, 2020, 17: 15.

[4] SMILLIE CS, BITON M, ORDOVAS-MONTANES J, et al. Intra- and inter-cellular rewiring of the human colon during ulcerative colitis. Cell, 2019, 178(3): 714–730.e22.

[5] LAVELLE A, SOKOL H. Gut microbiota-derived metabolites as key actors in inflammatory bowel disease. Nature Reviews Gastroenterology & Hepatology, 2020, 17(4): 223–237.

[6] SINGH S, MURAD MH, FUMERY M, et al. First- and second-line pharmacotherapies for patients with moderate to severely active ulcerative colitis: an updated network meta-analysis. Clinical Gastroenterology and Hepatology, 2020, 18(10): 2179–2191.e6.

[7] DA SILVA S, KEITA ÅV, MOHLIN S, et al. A novel topical PPARγ agonist induces PPARγ activity in ulcerative colitis mucosa and prevents and reverses inflammation in induced colitis models. Inflammatory Bowel Diseases, 2018, 24(4): 792–805.

[8] POUILLON L, TRAVIS S, BOSSUYT P, et al. Head-to-head trials in inflammatory bowel disease: past, present and future. Nature Reviews Gastroenterology & Hepatology, 2020, 17(6): 365–376

[9] GANJI-ARJENAKI M, RAFIEIAN-KOPAEI M. Phytotherapies in inflammatory bowel disease. Journal of Research in Medical Sciences, 2019, 24: 42.

[10] HE AM, CHADHA S, SARUCHI, et al. Phytocompound profiling and GC-MS analysis of *Lantana camara* leaf extract. Journal of the Indian Chemical Society, 2024, 101(11): 101379.

[11] SOUSA EO, MIRANDA CMBA, NOBRE CB, et al. Phytochemical analysis and antioxidant activities of *Lantana camara* and *Lantana montevidensis* extracts. Industrial Crops and Products, 2015, 70: 7–15.

[12] CHARAK SAMHITA. Vaidya Jadavaji Trikamji Acharya, Chakrapani with commentary. Bombay: Nirnaya Sagar Press, 1941.

[13] TAOUBI K, FAUVEL MT, GLEYE J, et al. Phenylpropanoid glycosides from *Lantana camara* and *Lippia multiflora*. Planta Medica, 1997, 63(2): 192–193.

[14] KIRTIKAR KR, BASU BD. Indian Medicinal Plants. Derhadun: International Book Distributors, 1981, 2: 1420–1423.

[15] GHISALBERTI EL. *Lantana camara* L. (Verbenaceae). Fitoterapia, 2000, 71(5): 467–486.

[16] DAY M, WILEY C, PLAYFORD J, et al. *Lantana*: current management status and future prospects. Canberra: Australian Centre for International Agricultural Research, 2003: 1–105.

[17] WU P, SONG ZT, WANG XL, et al. Bioactive triterpenoids from *Lantana camara* showing anti-inflammatory activities *in vitro* and *in vivo*. Bioorganic Chemistry, 2020, 101: 104004.

[18] SATHISH R, VYAWAHARE B, NATARAJAN K. Antiulcerogenic activity of *Lantana camara* leaves on gastric and duodenal ulcers in experimental rats. Journal of Ethnopharmacology, 2011, 134(1): 195–197.

[19] AMOAH V, ATAWUCHUGI P, JIBIRA Y, et al. *Lantana camara* leaf extract ameliorates memory deficit and the neuroinflammation associated with scopolamine-induced Alzheimer's-like cognitive impairment in zebrafish and mice. Pharmaceutical Biology, 2023, 61(1): 825–838.

[20] KHANDELWAL KR. Practical Pharmacognosy. Pune: Nirali Pakashan, 2007, 17: 149–159.

[21] MORRIS GP, BECK PL, HERRIDGE MS, et al. Hapten-induced model of chronic inflammation and ulceration in the rat colon. Gastroenterology, 1989, 96(3): 795–803.

[22] PORTER SN, HOWARTH GS, BUTLER RN. An orally administered growth factor extract derived from bovine whey suppresses breath ethane in colitic rats. Scandinavian Journal of Gastroenterology, 1998, 33(9): 967–974.

[23] BOBIN-DUBIGEON C, COLLIN X, GRIMAUD N, et al. Effects of tumour necrosis factor-α synthesis inhibitors on rat trinitrobenzene sulphonic acid-induced chronic colitis. European Journal of Pharmacology, 2001, 431(1): 103–110.

[24] MARKLUND S, MARKLUND G. Involvement of the superoxide anion radical in the autoxidation of pyrogallol and a convenient assay for superoxide dismutase. European Journal of Biochemistry, 1974, 47(3): 469–474.

[25] SEDLAK J, LINDSAY RH. Estimation of total, protein-bound, and nonprotein sulfhydryl groups in tissue with Ellman's reagent. Analytical Biochemistry, 1968, 25(1): 192–205.

[26] EBRAHIMPOUR S, FAZELI M, MEHRI S, et al. Boswellic acid improves cognitive function in a rat model through its antioxidant activity: neuroprotective effect of boswellic acid. Journal of Pharmacopuncture, 2017, 20(1): 10–17.

[27] SADAR SS, VYAWAHARE NS, BODHANKAR SL. Ferulic acid ameliorates TNBS-induced ulcerative colitis through modulation of cytokines, oxidative stress, iNOs, COX-2, and apoptosis in laboratory rats. EXCLI Journal, 2016, 15: 482–499.

[28] KRAWISZ JE, SHARON P, STENSON WF. Quantitative assay for acute intestinal inflammation based on myeloperoxidase activity. Assessment of inflammation in rat and Hamster models. Gastroenterology, 1984, 87(6): 1344–1350.

[29] GREEN LC, WAGNER DA, GLOGOWSKI J, et al. Analysis of nitrate, nitrite, and [15N] nitrate in biological fluids. Analytical Biochemistry, 1982, 126(1): 131–138.

[30] ARRIBAS B, SUÁREZ-PEREIRA E, ORTIZ MELLET C, et al. Di-D-fructose dianhydride-enriched caramels: effect on colon microbiota, inflammation, and tissue damage in trinitrobenzenesulfonic acid-induced colitic rats. Journal of Agricultural and Food Chemistry, 2010, 58(10): 6476–6484.

[31] SINGH UP, SINGH NP, BUSBEE B, et al. Alternative medicines as emerging therapies for inflammatory bowel diseases. International Reviews of Immunology, 2012, 31(1): 66–84.

[32] KONDAMUDI PK, MALAYANDI R, EAGA C, et al. Drugs as causative agents and therapeutic agents in inflammatory bowel disease. Acta Pharmaceutica Sinica B, 2013, 3(5): 289–296.

[33] JOSHI KS, NESARI TM, DEDGE AP, et al. Dosha phenotype specific Ayurveda intervention ameliorates asthma symptoms through cytokine modulations: results of whole system clinical trial. Journal of Ethnopharmacology, 2017, 197: 110–117.

[34] KANG GD, LIM S, KIM DH. Oleanolic acid ameliorates dextran sodium sulfate-induced colitis in mice by restoring the balance of Th17/Treg cells and inhibiting NF-κB signaling pathway. International Immunopharmacology, 2015, 29(2): 393–400.

[35] LIU BH, PIAO XH, GUO LY, et al. Ursolic acid protects against ulcerative colitis via anti-inflammatory and antioxidant effects in mice. Molecular Medicine Reports, 2016, 13(6): 4779–4785.

[36] XU B, LI YL, XU M, et al. Geniposide ameliorates TNBS-induced experimental colitis in rats via reducing inflammatory cytokine release and restoring impaired intestinal barrier function. Acta Pharmacologica Sinica, 2017, 38(5): 688–698.

[37] WAN F, CAI XY, WANG MY, et al. Chlorogenic acid supplementation alleviates dextran sulfate sodium (DSS)-induced colitis via inhibiting inflammatory responses and oxidative stress, improving gut barrier integrity and Nrf-2/HO-1 pathway. Journal of Functional Foods, 2021, 87: 104808.

[38] WANG TC, LIU XY, ZHANG WJ, et al. Traditional Chinese medicine treats ulcerative colitis by regulating gut microbiota, signaling pathway and cytokine: future novel method option for pharmacotherapy. Heliyon, 2024, 10(6): e27530.

[39] YANG YF, WANG Y, ZHAO L, et al. Chinese herbal medicines for treating ulcerative colitis via regulating gut microbiota-intestinal immunity axis. Chinese Herbal Medicines, 2023, 15(2): 181–200.

[40] ZHANG X, ZHANG L, CHAN JCP, et al. Chinese herbal medicines in the treatment of ulcerative colitis: a review. Chinese Medicine, 2022, 17(1): 43.

[41] ELBATREEK MH, FATHI AM, MAHDI I, et al. *Thymus satureioides* Coss. combats oral ulcer via inhibition of inflammation, proteolysis, and apoptosis. Inflammopharmacology, 2023, 31(5): 2557–2570.

[42] YADAV DK, MUDGAL V, AGRAWAL J, et al. Molecular docking and ADME studies of natural compounds of Agarwood oil for topical anti-inflammatory activity. Current Computer-Aided Drug Design, 2013, 9(3): 360–370.

[43] BRENNA Ø, FURNES MW, DROZDOV I, et al. Relevance of TNBS-colitis in rats: a methodological study with endoscopic, histologic and transcriptomic [corrected] characterization and correlation to IBD. PLoS One, 2013, 8(1): e54543.

[44] HAMBARDIKAR VR, MANDLIK DS. Protective effect of naringin ameliorates TNBS-induced colitis in rats via improving antioxidant status and pro-inflammatory cytokines. Immunopharmacology and Immunotoxicology, 2022, 44(3): 373–386.

[45] OWUSU G, OBIRI DD, AINOOSON GK, et al. Acetic acid-induced ulcerative colitis in sprague dawley rats is suppressed by hydroethanolic extract of *Cordia vignei* leaves through reduced serum levels of TNF-α and IL-6. International Journal of Chronic Diseases, 2020, 2020: 8785497.

[46] LEE SJ, SHIN JS, CHOI HE, et al. Chloroform fraction of *Solanum tuberosum* L. cv Jayoung epidermis suppresses LPS-induced inflammatory responses in macrophages and DSS-induced colitis in mice. Food and Chemical Toxicology, 2014, 63: 53–61.

[47] MANDLIK DS, MANDLIK SK, PATEL S. Protective effect of sarsasapogenin in TNBS induced ulcerative colitis in rats associated with downregulation of pro-inflammatory mediators and oxidative stress. Immunopharmacology and Immunotoxicology, 2021, 43(5): 571–583.

[48] STROBER W, FUSS IJ, BLUMBERG RS. The immunology of mucosal models of inflammation. Annual Review of Immunology, 2002, 20: 495–549.

[49] YAO JY, LU Y, ZHI M, et al. Inhibition of the interleukin-23/interleukin-17 pathway by anti-interleukin-23p19 monoclonal

antibody attenuates 2,4,6-trinitrobenzene sulfonic acid-induced Crohn's disease in rats. Molecular Medicine Reports, 2014, 10(4): 2105–2110.

[50] YU XY, LIU Y. Diosmetin attenuate experimental ulcerative colitis in rats via suppression of NF-κB, TNF-α and IL-6 signalling pathways correlated with down-regulation of apoptotic events. European Journal of Inflammation, 2021, 19: 20587392211067292.

[51] ADAKUDUGU EA, AMEYAW EO, OBESE E, et al. Protective effect of bergapten in acetic acid-induced colitis in rats. Heliyon, 2020, 6(8): e04710.

[52] ROGLER G, VAVRICKA S. *Anemia* in inflammatory bowel disease: an under-estimated problem? Frontiers in Medicine, 2015, 1: 58.

[53] GŁĄBSKA D, GUZEK D, KANAREK B, et al. Analysis of association between dietary intake and red blood cell count results in remission ulcerative colitis individuals. Medicina, 2019, 55(4): 96.

[54] MACK DR, SAUL B, BOYLE B, et al. Analysis of using the total white blood cell count to define severe new-onset ulcerative colitis in children. Journal of Pediatric Gastroenterology and Nutrition, 2020, 71(3): 354–360.

[55] JAISWAL S, MISHRA S, TORGAL SS, et al. Neuroprotective effect of epalrestat mediated through oxidative stress markers, cytokines and TAU protein levels in diabetic rats. Life Sciences, 2018, 207: 364–371.

[56] TIAN T, WANG ZL, ZHANG JH. Pathomechanisms of oxidative stress in inflammatory bowel disease and potential antioxidant therapies. Oxidative Medicine and Cellular Longevity, 2017, 2017: 4535194.

[57] MURAD HAS, ABDALLAH HM, ALI SS. *Mentha longifolia* protects against acetic-acid induced colitis in rats. Journal of Ethnopharmacology, 2016, 190: 354–361.

[58] LIU DY, GUAN YM, ZHAO HM, et al. The protective and healing effects of Sishen Wan in trinitrobenzene sulphonic acid-induced colitis. Journal of Ethnopharmacology, 2012, 143(2): 435–440.

[59] HANSBERRY DR, SHAH K, AGARWAL P, et al. Fecal myeloperoxidase as a biomarker for inflammatory bowel disease. Cureus, 2017, 9(1): e1004.

[60] KAMALIAN A, SOHRABI ASL M, DOLATSHAHI M, et al. Interventions of natural and synthetic agents in inflammatory bowel disease, modulation of nitric oxide pathways. World Journal of Gastroenterology, 2020, 26(24): 3365–3400.

[61] DE ZOETEN EF, FUSS IJ. Cytokines and inflammatory bowel disease. Pediatric Inflammatory Bowel Disease. Cham: Springer International Publishing, 2017: 31–43.

[62] FATANI AJ, ALROJAYEE FS, PARMAR MY, et al. *Myrrh* attenuates oxidative and inflammatory processes in acetic acid-induced ulcerative colitis. Experimental and Therapeutic Medicine, 2016, 12(2): 730–738.

[63] DINARELLO CA. Immunological and inflammatory functions of the interleukin-1 family. Annual Review of Immunology, 2009, 27: 519–550.

[64] AMINI-SHIRAZI N, HOSEINI A, RANJBAR A, et al. Inhibition of tumor necrosis factor and nitrosative/oxidative stresses by *Ziziphora* clinopoides (Kahlioti); a molecular mechanism of protection against dextran sodium sulfate-induced colitis in mice. Toxicology Mechanisms and Methods, 2009, 19(2): 183–189.

[65] SABBAH DA, HAJJO R, SWEIDAN K. Review on epidermal growth factor receptor (EGFR) structure, signaling pathways, interactions, and recent updates of EGFR inhibitors. Current Topics in Medicinal Chemistry, 2020, 20(10): 815–834.

[66] EL MAHDY RN, NADER MA, HELAL MG, et al. Eicosapentaenoic acid mitigates ulcerative colitis-induced by acetic acid through modulation of NF-κB and TGF-β/EGFR signaling pathways. Life Sciences, 2023, 327: 121820.

[67] AGGARWAL BB, KUNNUMAKKARA AB, HARIKUMAR KB, et al. Signal transducer and activator of transcription-3, inflammation, and cancer: how intimate is the relationship? Annals of the New York Academy of Sciences, 2009, 1171: 59–76.

[68] EDLICH F. BCL-2 proteins and apoptosis: recent insights and unknowns. Biochemical and Biophysical Research Communications, 2018, 500(1): 26–34.

马缨丹缓解 TNBS 诱导的大鼠溃疡性结肠炎：调控 TNF-α/EGFR/STAT3/Bcl-2 信号通路

Manoj S. Magre, Pooja A. Bhalerao, Satish K. Mandlik, Deepa S. Mandlik*

Bharati Vidyapeeth (Deemed to be University), Poona College of Pharmacy, Pune, Maharashtra 411038, India

【摘要】目的 探究马缨丹乙醇提取物（LCEE）对溃疡性结肠炎（UC）的治疗潜力及作用机制。**方法** 通过定性分析、液相色谱-质谱联用技术（LC-MS）及高效薄层色谱法（HPTLC）对 LCEE 进行植物化学成分分析。结合网络药理学分析筛选活性成分并预测靶点，随后进行分子对接。采用 2,4,6-三硝基苯磺酸（TNBS）诱导的 UC 大鼠模型（42 只雄性 Wistar 大鼠，200－250 g）验证其治疗机制。大鼠随机分为 7 组（每组 6 只）：正常对照组（NC）、乙醇对照组（EC）、疾病对照组（DC）、LCEE 低（100 mg/kg）、中（200 mg/kg）、高（400 mg/kg）剂量治疗组（口服）及地塞米松组（DEX，2 mg/kg，口服）。在 TNBS 诱导 UC（120 mg/kg，直肠给药）后，大鼠连续 28 天进行口服治疗。通过测量体重变化、疾病活动指数（DAI）、结肠重量/长度比及形态学评分评估疾病严重程度。检测血清及结肠组织中血液学参数、抗氧化酶（谷胱甘肽、超氧化物歧化酶、过氧化氢酶）、一氧化氮（NO）、髓过氧化物酶（MPO）及炎症细胞因子（TNF-α、IL-1β、NF-κB、IL-6、IL-12）水平。通过定量实时逆转录聚合酶链式反应（qRT-PCR）分析肿瘤坏死因子（TNF-α）、表皮生长因子受体（EGFR）、信号转导和转录激活因子（STAT3）及 B 细胞淋巴瘤（Bcl-2）的基因表达，并通过苏木素-伊红（HE）、吉萨姆染色、过碳酸-雪夫（PAS）染色评估结肠组织病理学变化。**结果** LC-MS 分析在 LCEE 中鉴定出 13 种植物化学成分，HPTLC 分析证实熊果酸、京尼平苷及绿原酸的存在。网络药理学筛选出 152 个潜在治疗靶点，其中 TNF、STAT3、Bcl-2、ALB 及 EGFR 为前 5 个核心靶点。分子对接显示，LCEE 成分与关键炎症及凋亡靶点具有较强的结合亲和力：苷类化合物与 TNF-α（－6.1 kcal/mol）、熊果酸与 STAT3（－6.8 kcal/mol）及 Bcl-2（－8.7 kcal/mol）、线蓟素与 EGFR（－8.2 kcal/mol），与 DEX 组相当。结果显示，LCEE 治疗可显著增加体重及胸腺重量，降低结肠重量、脾脏重量及 DAI 评分。血液学参数显示血红蛋白、红细胞及血小板计数显著升高，白细胞计数降低。抗氧化指标改善，谷胱甘肽、超氧化物歧化酶及过氧化氢酶水平升高，丙二醛水平下降。与 TNBS 组相比，LCEE 可显著降低 NO 和 MPO 水平及 TNF-α、IL-1β、NF-κB、IL-6、IL-12 等炎症因子水平。基因表达分析显示 LCEE 下调 TNF-α、EGFR 及 STAT3 表达，上调 Bcl-2 表达，表明其对炎症与凋亡通路的调控作用。组织病理学证实 LCEE 治疗后黏膜溃疡及炎性细胞浸润减少。**结论** 本研究结果表明，马缨丹可通过靶向 TNF-α/EGFR/STAT3/Bcl-2 信号通路缓解溃疡性结肠炎，为其临床应用提供了研究依据。

【关键词】溃疡性结肠炎；马缨丹；三硝基苯磺酸；网络药理学；分子对接；炎症细胞因子